# *Aspergillus fumigatus* can display persistence to the fungicidal drug voriconazole

Jennifer Scott[1#], Clara Valero[1,2#], Álvaro Mato-López[3], Ian J. Donaldson[4], Alejandra Roldán[3], Harry Chown[1], Norman Van Rhijn[1], Rebeca Lobo-Vega[3], Sara Gago[1], Takanori Furukawa[1], Alma Morogovsky[5], Ronen Ben Ami[5], Paul Bowyer[1], Nir Osherov[5], Thierry Fontaine[6], Gustavo H. Goldman[2], Emilia Mellado[3], Michael Bromley[1] and Jorge Amich[1,3,*].

1. Manchester Fungal Infection Group (MFIG), Division of Evolution, Infection, and Genomics, Faculty of Biology, Medicine and Health, University of Manchester, United Kingdom.
2. Faculdade de Ciências Farmacêuticas de Ribeirão Preto, Universidade de São Paulo, Ribeirão Preto, Brazil.
3. Mycology Reference Laboratory (Laboratorio de Referencia e Investigación en Micología LRIM), National Centre for Microbiology, Instituto de Salud Carlos III (ISCIII), Majadahonda, 28222 Madrid, Spain.
4. Bioinformatics Core Facility, Faculty of Biology, Medicine and Health, University of Manchester, United Kingdom.
5. Department of Clinical Microbiology and Immunology, Sackler School of Medicine Ramat-Aviv, Tel-Aviv. Sackler Faculty of Medicine, Tel Aviv University, Tel Aviv, Israel.
6. Institut Pasteur, Université de Paris, INRAE, USC2019, Unité Biologie et Pathogénicité Fongiques, F-75015, Paris, France.

# These authors contributed equally. They are ordered alphabetically

* Corresponding author: jamich@isciii.es

**ABSTRACT**

*Aspergillus fumigatus* is a filamentous fungus that can infect the lungs of patients with immunosuppression and/or underlying lung-diseases. The mortality associated with chronic and invasive aspergillosis infections remain very high, despite availability of antifungal treatments. In the last decade, there has been a worrisome emergence and spread of resistance to the first line antifungals, the azoles. The mortality caused by resistant isolates is even higher, and patient management is complicated as the therapeutic options are reduced. Nevertheless, treatment failure is also common in patients infected with azole-susceptible isolates, which can be due to several non-mutually exclusive reasons, such as poor drug absorption. In addition, the phenomena of tolerance or persistence, where susceptible pathogens can survive the action of an antimicrobial for extended periods, have been associated with treatment failure in bacterial infections, and their occurrence in fungal infections already proposed. Here, we demonstrate that some isolates of *A. fumigatus* display persistence to voriconazole. A sub-population of the persister isolates can survive for extended periods and even grow at slow rates in the presence of supra-MIC (Minimum Inhibitory Concentration) of voriconazole and seemingly other azoles. Persistence cannot be eradicated with adjuvant drugs or antifungal combinations and seems to reduce the efficacy of treatment for certain individuals in a *Galleria mellonella* model of infection. Furthermore, persistence implies a distinct transcriptional profile, demonstrating that it is an active response. We propose that azole persistence might be a relevant and underestimated factor that could influence the outcome of infection in human aspergillosis.

**IMPORTANCE**

The phenomena of antibacterial tolerance and persistence, where pathogenic microbes can survive for extended periods in the presence of cidal drug concentrations, have received significant attention in the last decade. Several mechanisms of action have been elucidated, and their relevance for treatment failure in bacterial infections demonstrated. In contrast, our knowledge about antifungal tolerance and, particularly, persistence are still very scarce. In this study, we have characterised the response of the prominent fungal pathogen *Aspergillus fumigatus* to the first line therapy antifungal voriconazole. We comprehensively show that some isolates display persistence to this fungicidal antifungal and identify various potential mechanisms of action. In addition, using an alternative model of infection, we provide initial evidence to suggest that persistence may cause treatment failure in some individuals. Therefore, we propose that azole persistence is an important factor to consider and further investigate in *A. fumigatus*.

63 **INTRODUCTION**

64 *Aspergillus fumigatus* is the most prominent fungal pathogen of the human lung, being the major
65 causative agent of a range of diseases collectively termed aspergillosis [1]. The incidence of fatal
66 aspergillosis infections is on the rise due to the increase in the at-risk population [2, 3], including
67 severe COVID-19 patients [4-6]. The mortality associated with *A. fumigatus* infections remains
68 unacceptably high: 38% 5-year mortality rates for chronic pulmonary aspergillosis [7] and ranging from
69 ~35% in early diagnosed and treated patients to nearly 100% if diagnosis is missed or delayed in
70 invasive aspergillosis [8]. These number represent the highest mortality of all invasive fungal diseases
71 [9]. This situation has become even more worrisome due to the emergence of clinical resistance to
72 existing antifungals, which poses a serious threat to human health [10]. Azoles are currently the only
73 FDA-approved class of mould-active agents that can be administrated orally and intravenously, and
74 accordingly they are used for both the evidence-based treatment and prevention of aspergillosis
75 diseases [11]. However, in the last decade, the number of clinical *A. fumigatus* isolates that are
76 resistant to triazole drugs has increased worldwide, causing serious problems for clinical management,
77 as the therapeutic options are reduced and the mortality rates caused by resistant isolates are higher
78 [7, 12, 13]. Furthermore, both in clinical disease and in experimental animal models, it has been
79 observed that treatment failure is common even if the infecting fungal isolate is susceptible to the
80 azole used for treatment [14, 15]. There are several possible explanations for treatment failure in
81 these cases, including antifungal tolerance or persistence [16, 17].

82 In the last decade there has been a revolution in our understanding of how pathogenic
83 microorganisms withstand the challenge of antimicrobial drugs. Classically, pathogens were described
84 to be either susceptible or resistant to a certain drug. Antimicrobial resistance is due to a genetic
85 feature in the microbe (intrinsic or acquired *via* mutations) that enables it to grow normally at high
86 concentrations of the agent, above the Minimum Inhibitory Concentration (MIC) defined for the
87 antimicrobial based on the clinical breakpoint. However, in recent years it has become obvious that
88 microbes can withstand the action of drugs by at least three other mechanisms: tolerance,
89 persistence, or heteroresistance. These three phenomena share the feature that they are not
90 triggered by mutations in the microbe's DNA sequence, yet differ in other details. Drug tolerance has
91 been defined as the ability of all cells of a genetically isogenic strain to survive, and even grow at slow
92 rates, for extended periods in the presence of drug concentrations that are greater than the minimal
93 inhibitory concentration (MIC). In persistence, only a small fraction of the isogenic population (usually
94 <1% of the cells) survive, and grow at slow rates, for an extended period of time in the presence of
95 supra-MIC concentrations of the drug [18, 19]. These two phenomena do not imply an increase in the
96 MIC. Finally, heteroresistance is the transient capacity of a microbial subpopulation to increase the

97 MIC in the presence of the drug, due to adaptation, epigenetic modifications or reversible aneuploidy.
98 All those phenomena have been implicated in treatment failure and relapse in bacterial infections [18,
99 20]. These definitions are summarised in Table 1.

| Phenomenon | Previous (bacteria) Definition | Adjustment for Fungi |
|---|---|---|
| **Resistance** | Stable capacity of an isolate to grow normally in the presence of high concentrations of the drug, above the minimum inhibitory concentration (MIC) defined for the antimicrobial based on the clinical breakpoint. This capacity is based on specific genetic sequence(s) (intrinsic or acquired) in the genome. | The same definition for fungi |
| **Heteroresistance** | Transient capacity of a subpopulation of cells to increase the MIC in the presence of the drug, without a modification in the genome sequence. | The same definition for fungi |
| **Tolerance** | Ability of all cells of a susceptible, genetically isogenic strain to survive, and even grow at slow rates, for extended periods in the presence of drug concentrations that are greater than the MIC. | In the presence of fungistatic drugs, capacity of all or high proportion of the cells of a susceptible isolate to grow in the presence of drug concentrations that are greater than the MIC. |
| **Persistence** | Ability of a small subpopulation of cells of a susceptible, genetically isogenic strain to survive, and even grow at slow rates, for extended periods in the presence of drug concentrations that are greater than the MIC. | In the presence of fungicidal drugs, capacity of a small fraction of cells of a susceptible isolate to survive, and even grow at slow rates, for extended periods in the presence of drug concentrations that are greater than the MIC. |

100

101 **Table 1**. Current and proposed definitions for the phenomena of resistance, heteroresistance,
102 tolerance and persistence in pathogenic fungi (see discussion).

103

104 In fungi, tolerance has been often described as “trailing growth” and its relevance for infection has
105 been mostly disregarded. However, a recent landmark study in *Candida albicans* has characterised
106 tolerance as a distinct, strain-specific feature and provided evidence for its relevance in persistent
107 candidemia [17, 21]. In *Aspergillus*, trailing growth is known to be prominent in the presence of
108 caspofungin [22, 23] apparently due to single strain heterogeneity [24]. Moreover, at higher
109 concentrations of this drug some isolates can resume normal growth, an effect known as “Eagle” or
110 paradoxical effect (see review [25] for more information), which we have recently demonstrated as a
111 tolerance phenotype [26]. The possible relevance of the paradoxical effect in clinical practice is still
112 under debate, but there is evidence suggesting that it might be important [27], and concern has been

113 raised by some clinicians [28]. Remarkably, it seems that the phenomenon of tolerance in fungi is seen
114 with static drugs, e.g. azoles for *C. albicans* and echinocandins for *A. fumigatus*. However, the
115 possibility that *A. fumigatus* can display tolerance or persistence to azole antifungals had not been
116 previously investigated. Interestingly, in contrast to *C. albicans* and *Cryptococcus neoformans*, azoles
117 have been shown to have fungicidal activity against *A. fumigatus* [29-31], which implies that the
118 underlying mechanisms are likely different. Whilst these phenomena have so far only been
119 investigated in bacteria or yeasts, the approaches to detect and investigate azole tolerance or
120 persistence need to be tailored in filamentous fungi, like *A. fumigatus*, as these organisms form
121 multicellular hyphae. Using various complementary approaches, here we show that small
122 subpopulations of certain *A. fumigatus* isolates can survive and even grow at slow rates at supra-MIC
123 concentrations of the fungicidal drug voriconazole.

124

125 **RESULTS**

126 **Some *Aspergillus fumigatus* isolates show persistence to voriconazole**

127 To determine whether *A. fumigatus* can display tolerance or persistence to voriconazole, we examined
128 a collection of isolates consisting of 9 environmental, 10 clinical (gift from Prof Paul Dyer, collection
129 PD-47-XX, here shortened as PD-XX), 5 common laboratory strains and one resistant control (RC)
130 harbouring the TR34/L98H mutations in the *cyp51A* locus (Table S1 in
131 https://doi.org/10.5281/zenodo.7021623), using disc diffusion assays. We evenly spread $4\times10^4$
132 conidia of the isolates on RPMI agar plates, placed a 6 mm disc in the centre, containing 10 µL of
133 voriconazole (0.8 mg/mL), and incubated them for 5 days. We observed variability in the sizes of the
134 inhibition halos, reflecting differences in susceptibility of the isolates (Figs. 1A and S1). As expected,
135 the RC strain did not show a proper inhibition halo (Figs. 1A and S1). In contrast, 15 of the 20 isolates
136 showed a clear and well-defined inhibition zone. Interestingly, we found that 5 isolates were able to
137 form colonies within the halo of inhibition, and 4 in 5 of these isolates (PD-9, PD-104, PD-254 and PD-
138 266, Fig. S1) formed only a few small colonies, which might be indicative that a few conidia are able
139 to germinate and grow a little in the presence of a supra-MIC concentration of voriconazole (Fig. 1A
140 and S1). The remaining isolate (PD-256) did not show any inhibition halo, suggesting that it is a
141 resistant isolate.

142 We then assessed the MICs of the original isolates and their derived colonies of the halo (CoHs). A
143 complication of working with a filamentous fungus is that the CoHs need to be grown on a new plate
144 in order to harvest spores (conidia) to be used for MIC determination. We therefore decided to assay
145 two different conidia-harvesting conditions to distinguish the different phenotypes: re-growing the

146 CoHs on solid RPMI in the absence or in the presence of a low concentration of voriconazole (0.12
147 µg/mL). It would be expected that for conidia grown in the presence of the drug, both resistance and
148 heteroresistance are detected as an increment in the isolate's MIC. In contrast, for conidia grown in
149 the absence of the drug, the reversible increase in MIC that is characteristic of heteroresistance would
150 be lost, whilst a stable genetic-based increment in MIC that defines resistance would be maintained.
151 Finally, persistence should not cause a change of the isolate's MIC independently of the presence of
152 the drug in the conidia-harvesting medium. Using conidia obtained from both conditions, absence and
153 presence of voriconazole, we found that the original isolate did not show an inhibition halo (PD-256,
154 Fig. 1A and S1) had a very high MIC (>8 µg/mL), demonstrating that it is a resistant isolate (Table 2).
155 CoHs formed by PD-254 and PD-266, which upon re-inoculation did not show an inhibition halo (Fig.
156 S1), showed an increased MIC compared to the parental isolate (Table 2). The colony picked from PD-
157 254 showed increased MIC when re-grown on both media with and without voriconazole, suggesting
158 that the CoH may have acquired a mutation that confers a stable resistance phenotype. In contrast,
159 PD-266, which already had an elevated MIC, only showed an increased MIC when re-grown on medium
160 containing voriconazole, suggesting that this strain may be heteroresistant. Finally, CoHs from isolates
161 PD-9 and PD-104 showed the same MICs as their original isolates after a passage in the absence or
162 presence of voriconazole (Table 2). This suggests that they are not resistant or heteroresistant
163 derivatives of the original isolates. Indeed, repetition of the disc assay with the original isolates and
164 with CoH re-grown in the presence of voriconazole, showed a similar level of colony appearance in
165 the original strains and their derived CoHs for PD-9 and PD-104 (whereas it grew to the edge of the
166 disc for PD-266, reflecting again a transient increase in its MIC) (Fig. S1). Although no formal
167 measurement of growth rate was performed, the clear difference in size between single persister (PD-
168 9 and PD-104) and heteroresistant colonies (PD-266) after the same time of incubation (Fig. S1)
169 indicate that the growth rate of persister colonies is reduced. Interestingly, all isolates showed a small
170 increase (one dilution) in MIC when re-grown in the presence of drug (Table 2). This may be due to
171 the development of conidia adapted to the growing environment in preparation for the subsequent
172 germination, an effect recently described in *Aspergillus spp* [32]. Next, we tested if CoHs could also be
173 detected using E-tests strips, which is a well-established method to measure the MIC and is thus more
174 quantitative than disc diffusion assay [33]. In agreement with disc diffusion assays, CoHs developed
175 inside the halo of inhibition created by E-tests on persister isolates (PD-9 and PD-104), but not on non-
176 persister isolates (ATCC and PD-60) (Fig. S2A). Finally, to verify that the persistence phenotype is
177 stable, we sequentially passaged CoHs isolated from PD-9 and PD-104 on PDA media (without
178 voriconazole) and performed disc diffusion assays every two/three passages. The halo of the disc and

179 the relative level of persistence were maintained for 10 passages (Fig. S2B), demonstrating that
180 persistence is a stable phenotype.

181

| | Voriconazole MIC (µg/mL) | | | | |
|---|---|---|---|---|---|
| **Isolate** | **original** | **Original (grown on Drug)** | **CoH (- Drug)** | **CoH (grown on Drug)** | **Classification of CoH** |
| ATCC | 1 | 2 | | | Susceptible |
| PD-9* | 0.5 | 1 | 0.5 | 1 | Persister |
| PD-104* | 1 | 2 | 1 | 2 | Persister |
| PD-254 | 2 | 2 | >8 | >8 | Resistant |
| PD-256 | >8 | >8 | >8 | >8 | Resistant |
| PD-266 | 4 | 8 | 4 | >8 | Heteroresistant |

182 **Table 2**. Voriconazole MICs of original isolates and their derived CoHs, pre-grown both in the absence
183 and presence of a low (0.12 µg/mL) concentration of voriconazole

184

185 In bacteria, persister and tolerant cells are often dormant and do not grow [19]. To investigate this in
186 *A. fumigatus* in more detail, we followed a protocol to detect tolerance/persistence in bacteria in
187 which the disc containing the drug, after a period of incubation, is switched, with another one
188 containing fresh media [34]. The rationale is to detect surviving cells that have remained dormant and
189 resume growth after the drug is withdrawn. After initial growth we substituted the disc with
190 voriconazole for a new one containing *Aspergillus* Minimal Media (AMM). Interestingly, after the disc
191 switch colonies were observed in the halos for several isolates (CEA10, PD-7, -8, -50, -154, -249, and -
192 264, Fig. S3), suggesting that these may be low level persister isolates. Nevertheless, three isolates,
193 PD-9, -104 and -259, were able to form colonies before the disc switch, and of these three, only PD-9
194 and PD-104 grew even more colonies after disc switch (Fig. S3). Therefore, the isolates PD-9 and PD-
195 104 were able to survive and grow at slower rates in the presence of supra-MIC concentrations of
196 voriconazole, a phenomenon that complies with the definition of persistence.

197 To further characterize persistence in *A. fumigatus*, we performed MIC assays with selected strains
198 and checked microscopic growth of persister and non-persister isolates at supra-MIC concentrations.
199 We found that 72 hours after inoculation the non-persister strains ATCC46645 and PD-60 displayed
200 microscopic growth only at the MIC concentration, and no growth at all at higher concentrations (Figs.
201 1B and S4). In contrast, the persister isolates PD-9 and -104 showed noticeable microscopic growth at
202 2X, and even at 3X MIC germinated conidia could be detected (Fig. 1B and S4). While the level of
203 growth was variable among independent experiments, the difference between persister and non-
204 persister isolates was consistently observed (Fig. 1B and S4). In addition, we plated the entire content
205 of the wells containing the highest concentrations of voriconazole (8 µg/mL) and found that 48 h after

206 inoculation the non-persister strains were nearly all killed (only ~0.07% of the conidia survived) whilst
207 in the persister strains a significantly higher ratio of conidia survived (0.39% of PD-9 $p$=0.002 and 0.18%
208 of PD-104 $p$=0.0331, Fig. 1C). Therefore, a subpopulation of the *A. fumigatus* persister isolates can
209 survive for long periods in the presence of high concentrations of voriconazole and even grow at a
210 slow rate, which seem to be inversely correlated with the concentration of drug.

211 In bacteria, a combination of MIC and speed of killing is the best approach to reveal and differentiate
212 tolerance and persistence [18]. Therefore, we investigated the dynamics of cell death caused by
213 voriconazole for persister and non-persister isolates. Conidia from two susceptible (ATCC46645 and
214 PD-60), two persister (PD-9 and PD-104) and the putative heteroresistant (PD-266) strains were
215 incubated for 4 days in liquid RPMI in the presence of 4 µg/mL of voriconazole and aliquots of the
216 culture plated (after PBS washing to remove the drug) on PDA rich media every 24 hours (Fig. 1D). We
217 found that for all strains the number of viable conidia dramatically declined after 24 hours of
218 incubation, reflecting a strong fungicidal action of voriconazole, even against an isolate with high MIC.
219 Interestingly, whilst the susceptible isolates were completely killed within 48-72 hours, a considerable
220 number of conidia from the persister strains maintained viability for an extended period (~0.748% for
221 PD-9, ~0.136% for PD-9 at 48 h and ~0.52% for PD-9, ~0.128% for PD-9 at 72 h, Fig. 1D), resulting in
222 the characteristic biphasic killing curve that is the hallmark of persistence [19]. The isolate PD-266
223 showed visible growth from 48h, which agrees with its proposed heteroresistant phenotype, and
224 saturated the plate, making impossible to count colony forming units (CFUs). To investigate the
225 survival of the isolates at the single cell (conidial) level, we incubated the two persister and one
226 susceptible strains in liquid RPMI in the presence of 32 µg/mL voriconazole for 48 hours, and replaced
227 it with fresh drug free medium. We observed that during the first 24 hours of incubation after drug
228 withdrawal there was no growth for any of the isolates, but subsequently the persister strains were
229 able to resume growth (Videos S1 and S2 in https://doi.org/10.5281/zenodo.7021623) whilst the
230 susceptible strain was not (Video S3 in https://doi.org/10.5281/zenodo.7021623). Hence, persister
231 strains indeed can survive for extended periods in the presence of high concentrations of voriconazole
232 and resume growth when the drug is withdrawn.

233 To check if the observed phenomena could be explained by mutations in the azole target genes, we
234 sequenced the promoter and ORF of *cyp51A* and the ORF of *cyp51B* in the persister isolates PD-9 and
235 PD-104 and the non-persister strain PD-60. In all strains we found that *cyp51A* was completely wild-
236 type (there were no nucleotide changes) and *cyp51B* had only synonymous polymorphisms (Table S2
237 in https://doi.org/10.5281/zenodo.7021623), thus denying an implication of target enzyme mutations
238 in the phenomenon of persistence. We also sequenced the sterol-sensing domain of *hmg1*, as it has
239 been proposed that mutations in this gene may be a precursor step for the development of azole

240 resistance [35, 36], and in bacteria persistence has been shown to correlate with the evolution of
241 resistance [37, 38]. However, we found again that all strains harboured a completely wild-type
242 sequence (not shown), suggesting that *hmg1* is not related with voriconazole persistence.

243 In conclusion, we have observed that certain *A. fumigatus* isolates can survive and grow at slow rates
244 for extended periods of time in the presence of supra-MIC concentrations of voriconazole, therefore,
245 these isolates display persistence to voriconazole.

Fig. 1

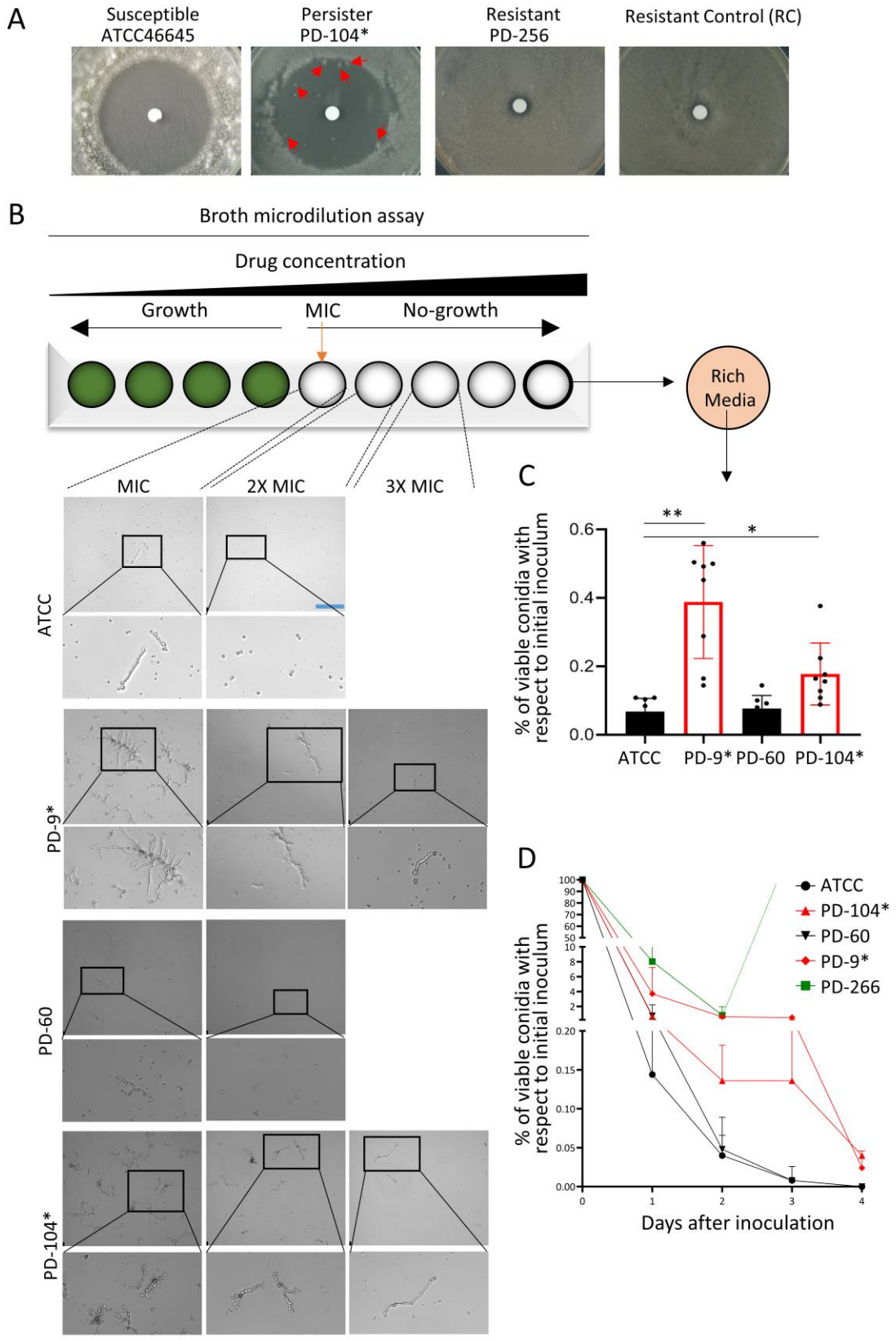


246

247

248

249 **Figure 1. Certain *Aspergillus fumigatus* isolates display persistence to voriconazole.**

250 **A)** In disc-diffusion assays (10 µL of 0.8 mg/mL voriconazole), the susceptible isolate ATCC46645 never
251 grew any colony in the inhibition halo, the resistant control (RC) isolate grew up to the edge of the
252 disc, as did the strain PD-256. The persister isolate PD-104 was consistently able to grow a few small
253 colonies. Plates were incubated for 5 days at 37°C. **B)** Inspection of the wells of a broth dilution assay
254 under the microscope 72 hours after inoculation revealed that the non-persister isolates ATCC and
255 PD-60 displayed only limited microscopic growth at the MIC concentration, and all conidia remained
256 non-germinated at higher concentrations. In contrast, the persister strains PD-9 and PD-104 showed
257 noticeable microscopic growth up to three fold (3x) the MIC concentration. Scale bar= 132.5 µm. **C)**
258 Full content of the well containing the maximum concentration of voriconazole (8 µg/mL) was plated
259 on rich media PDA plates and (CFUs) counted 48 hours after inoculation. Persister isolates grew
260 significantly more CFUs than non-persister isolates (PD-9 VS ATC46645C $p$=0.002 and PD-104 VS
261 ATCC46645 $p$=0.0331), demonstrating that these strains remain viable upon azole treatment for a
262 longer period. Three independent experiments with three biological replicates were performed, the
263 graph represents the means and SD, and data was analysed using the Brown-Forsythe and Welch
264 ANOVA test with Dunnett's multiple comparisons. **D)** A survival curve in the presence of 4 µg/mL of
265 voriconazole revealed that, whilst non-persister strains lost viability very rapidly, the persister isolates
266 had the characteristic bi-phasic reduction in viability, showing that a sub-population of the persister
267 isolates remained viable for a longer period. Two independent experiments with biological duplicates
268 and two technical replicates were performed; the graph represents the means and SD.

269

270

271 ***Aspergillus fumigatus* persistence is maintained in the hyphal transition and seems to be medium**
272 **dependent.**

273 *A. fumigatus* undergoes morphological changes during its development, shifting from resting conidia
274 to swollen conidia (~4-5 h), then to germlings (~8 h) and finally forming hyphae (~16 h) (Fig. S5A). As
275 the cellular metabolic status is different at each developmental stage [39-41], we speculated that it
276 might influence the capacity of the fungus to deploy persistence in the presence of voriconazole.
277 Initially, to rule out that persistence could be explained by basal differences in germination or growth,
278 we examined the germination and growth rates of two persister (PD-9 and PD-104) and two non-
279 persister (ATCC and PD-60) isolates. We found that all isolates germinated at equivalent rate and ratio
280 (Fig. S5B) and grew similarly on both solid (Fig S5C) and liquid (Fig. S5D) RPMI media. Once excluded
281 differences in germination or growth, we tested the influence of the morphological stage on
282 persistence by incubating the RPMI plates inoculated with the fungus for 8 or 16 hours before adding
283 the drug to the disc. We found that the persister strains PD-9 and PD-104 were also able to form
284 colonies in the halo when drug was added 8 hours after the beginning of incubation (Fig. 2A),
285 suggesting that persistence is not determined by the developmental stage. We could not draw
286 definitive conclusions for the 16 hours grown hyphae, as the background growth was too dense to
287 undoubtedly differentiate specific persister colonies (Fig. 2A). Nevertheless, we could clearly detect a
288 growing colony in the voriconazole halo for the strain PD-104 (Fig. 2A), proving that at least this strain

289 can display persister growth when short hyphae are challenged with the drug. Interestingly, it has
290 previously been reported that morphological status alters *A. fumigatus* susceptibility profiles against
291 various drugs including voriconazole [42], which supports the notion that persistence is a different
292 phenomenon, triggered by distinct mechanisms, and independent of MIC.

293 To determine if persistence is influenced by the growth medium, we performed a voriconazole disc
294 diffusion assay with the PD-104 isolate and the wild-type control ATCC46645 on PDA rich media or
295 AMM. The PD-104 strain showed persister growth on both media, and it seemed to be able to form a
296 higher number of COHs on PDA rich media (Fig. 2B). The ATCC46645 wild-type strain did not show
297 persistence on AMM, but surprisingly it did form colonies in the halo on PDA media (Fig. 2B). To
298 investigate this in more detail we repeated the disc assay using two different rich media, PDA and
299 Sabouraud, with more strains, CEA10, PD-9, and PD-60 (Fig. 2C) and found that all strains were able
300 to form colonies in the halos. The MICs of the isolates, measured by broth dilution assay, were equal
301 on Sabouraud and RPMI (Fig. 2D), indicating that the effect of the drug is not reduced in rich medium.
302 Therefore, the ability of *A. fumigatus* to display persistence seems to be medium dependent,
303 suggesting that a rich nutrient environment favours survival at supra-MIC concentrations. This is
304 supported by a recent study that showed that a rich metabolic environment can promote azole
305 tolerance in *Saccharomyces cerevisiae* [43]. Nevertheless, it should also be considered that
306 voriconazole diffusion may be affected in solid rich media, which could be confounding this
307 observation.

308 Finally, we also considered that persistence might be affected by the age of the spores (all experiments
309 are performed with freshly harvested spores). To check this, we assayed disc diffusion assays using
310 10-weeks old spores. We did not observe remarkable differences with respect to fresh spores,
311 although in most of the experiments we could see one colony in the halo of the non-persister PD-60
312 (Fig. 2E), suggesting that aged spores might have a slightly higher persistence potential, at least for
313 some isolates.

Fig. 2

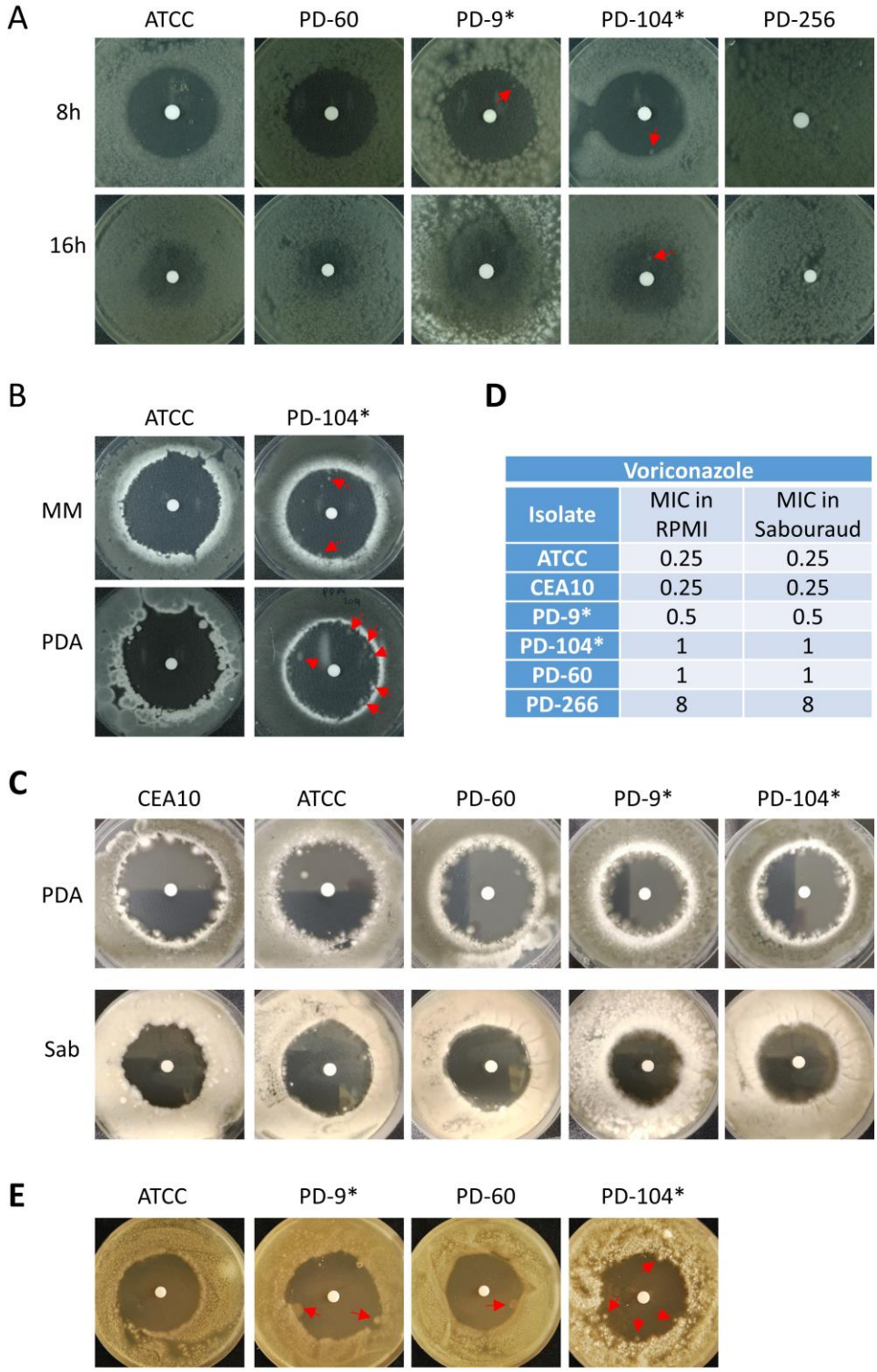


D

| Voriconazole | | |
|---|---|---|
| Isolate | MIC in RPMI | MIC in Sabouraud |
| ATCC | 0.25 | 0.25 |
| CEA10 | 0.25 | 0.25 |
| PD-9* | 0.5 | 0.5 |
| PD-104* | 1 | 1 |
| PD-60 | 1 | 1 |
| PD-266 | 8 | 8 |

**Figure 2. *Aspergillus fumigatus* persistence does not depend on the morphological stage, but seems to be determined by the growth media**.

**A)** Conidia of the different isolates were inoculated and incubated for 8 or 16 hours before the disc containing voriconazole (10 µL of 0.8 mg/mL) was added to the RPMI plate. At 8 hours, when conidia have germinated, the persister isolates PD-9 and PD-104 were still able to grow small colonies in the inhibition halo, whilst the non-persister strains were not. At 16 hours, when conidia have already

321 formed hyphae, the background growth made impossible to distinguish colonies in PD-9, but a clear
322 one could be detected in PD-104. **B)** On *Aspergillus* minimal medium (MM), the persister isolate PD-
323 104 was able to form colonies in the halo, but the non-persister strain ATCC was not. **C)** On rich media
324 PDA and Sabouraud (Sab) all isolates were able to form conidia in the halo. **D)** This happened even the
325 MIC of all isolates was the same in commonly assayed RPMI and the rich media Sab. **E)** 10-week old
326 spores displayed a similar persister phenotype as freshly isolated spores. Often a single colony could
327 be detected in the halo of inhibition on the non-persister PD-60, suggesting that aged spores might
328 have slightly more persistence capacity.

329

330 ***Aspergillus fumigatus* persistence to voriconazole is independent of stress and cannot be inhibited**
331 **with adjuvant or antifungal drugs.**

332 Changing environmental conditions activate signalling cascades that trigger transcriptional adaptation
333 and cell wall alterations [44-47]. Therefore, we reasoned that the capacity of certain isolates to survive
334 and grow in supra-MIC concentrations of voriconazole might be influenced by environmental
335 stressors. Indeed, in *C. albicans* mutants and inhibitors of stress response pathways eliminate
336 tolerance [48]. To investigate this possibility, we analysed voriconazole persistence of PD-104 in the
337 presence of hypoxic (1% $O_2$), oxidative (0.01% $H_2O_2$), osmotic (150 mM NaCl), membrane (0.05% SDS)
338 and cell wall (10 µg/mL CalcoFluor White) stress. Surprisingly, in contrast to *C. albicans* [21], we found
339 that most environmental conditions did not influence persistence in *A. fumigatus* (Fig. 3A). This
340 suggests that the underlying mechanism(s) of persistence in *A. fumigatus* are likely different from the
341 previously proposed mechanisms of tolerance in *C. albicans*. The only condition that influenced *A.*
342 *fumigatus* persistence was hypoxia, which could prevent growth in the halo (Fig. 3A). As we had
343 observed above that persistence was influenced by the growth medium, we wondered if hypoxia could
344 prevent persistence also on rich medium. As shown in Figs. 2B and 2C, all isolates were able to grow
345 colonies in the halo when grown on the rich medium YAG on normoxia (Fig. 3B). However, persistence
346 was eliminated under hypoxia for all strains, except for PD-104, for which it was reduced but
347 apparently not completely eradicated. Therefore, it seems that hypoxia reduces persistence, but the
348 nutritional composition of the medium also influences its impact on the phenomenon.

349 In *C. albicans*, fluconazole tolerance (but not resistance) can be prevented with the use of adjuvant
350 drugs that block general stress signalling pathways [21]. To further investigate if the underlying
351 mechanism of persistence may be different in *A. fumigatus*, we tested the effect of various drug
352 adjuvants that were previously shown to eliminate tolerance in *C. albicans* [21]: geldanamycin (0.8
353 µg/mL), an inhibitor of heat shock protein (Hsp90) [49, 50], FK506 (4 ng/mL), an inhibitor of calcineurin
354 [51], H-89 (4 µg/mL), an inhibitor of the cAMP-dependent protein kinase (PKA) [52], rapamycin (6.25
355 µg/mL), an inhibitor of the mammalian target of rapamycin (mTOR) [53], and tunicamycin (10 µg/mL),
356 an inducer of the unfolded protein response pathway [54]. In contrast to *C. albicans*, the use of

357 adjuvant drugs did not prevent persistence of *A. fumigatus* isolates (Fig. 3C). We also tested lovastatin
358 (8 µg/mL) and simvastatin (2 µg/mL), as statins inhibit 3-hydroxy-3-methylglutaryl-coenzyme A
359 (HmgA) [55], an enzyme in the same metabolic pathway as the target of azoles, and these two were
360 previously shown to have antifungal activity against *Aspergillus spp* [56]. However, statins were also
361 not able to prevent persister growth (Fig. 3B). Finally, as efflux of antifungals has been proposed to
362 play a role in *C. albicans* tolerance [48], we tested if the efflux inhibitors milbemycin A oxim (8 µg/mL)
363 [57] or clorgyline (63.5 µg/mL) [58] can prevent *A. fumigatus* persistence. These compounds seemed
364 to be able to diminish the persister capacity of the strains, as only one CoH per plate could be detected,
365 and these colonies were exactly at the edge of the halo (Fig. 3C). In conclusion, adjuvant drugs cannot
366 prevent *A. fumigatus* persistence to voriconazole, and efflux inhibitors may affect this process and
367 deserve further study.

368 Next, we evaluated if persistence can be eradicated using combinatorial treatment with the other
369 classes of antifungal drugs in clinical use. However, neither amphotericin-B (1 µg/mL) nor caspofungin
370 (0.5 µg/mL) could prevent persistence (Fig. 3D). Interestingly, these antifungal drugs could also not
371 impede growth in the halo of the presumed heteroresistant strain PD-266 (Fig. 3D). Therefore, it
372 seems that combinatorial treatment with other antifungals cannot prevent persistence in *A.*
373 *fumigatus*.

Fig. 3

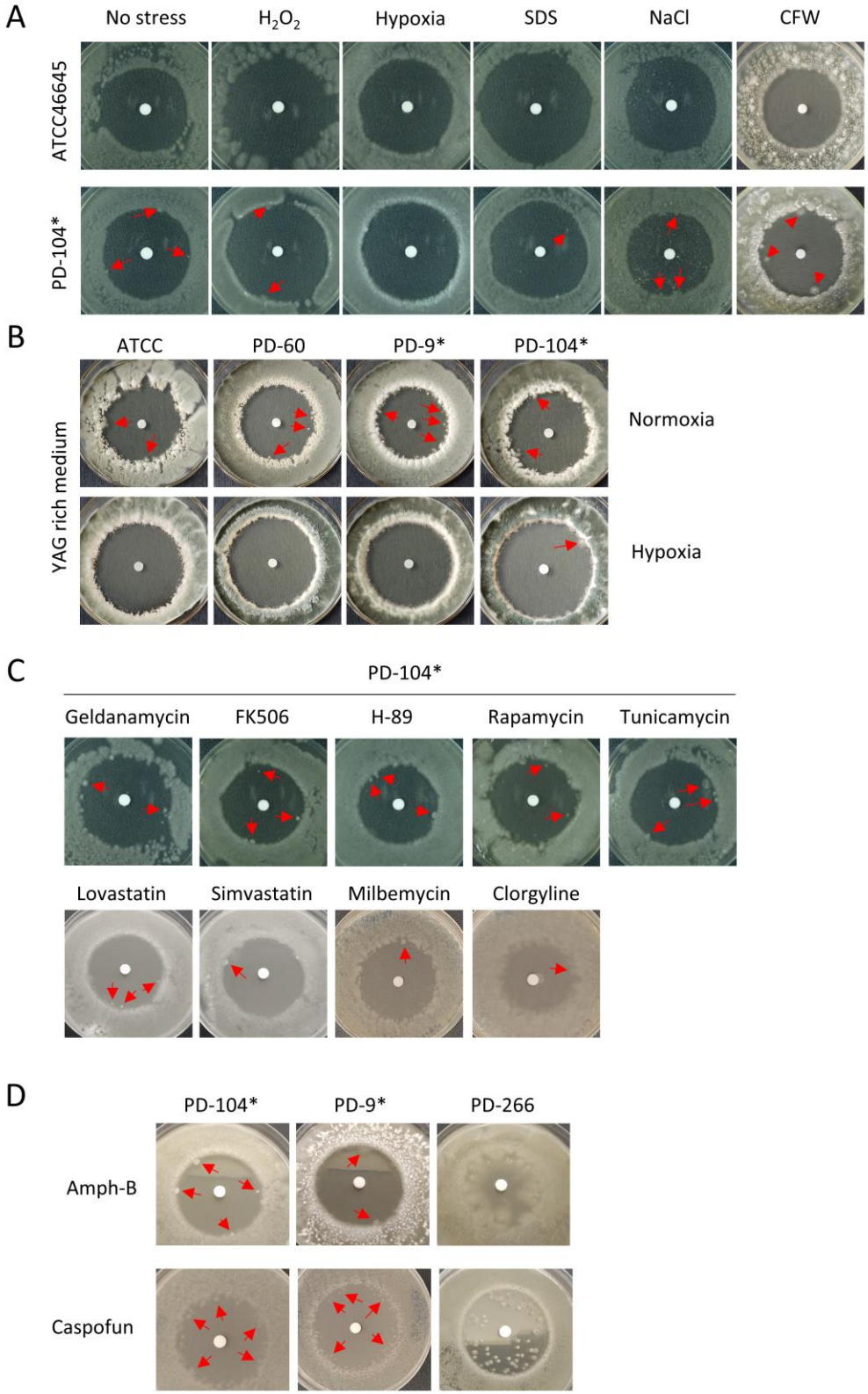


374

375 **Figure 3. *Aspergillus fumigatus* persistence is not influenced by stress, with the exception of**
376 **hypoxia, and cannot be eliminated with adjuvant or combinatorial treatments.**

377 **A)** Hypoxia was the only stress that could prevent persistence, whilst neither oxidative ($H_2O_2$), cell wall
378 (SDS or CFW) or osmotic (NaCl) stress influenced persistence. **B)** Hypoxia completely eradicated

379 persistence also on the rich medium YAG for ATCC, PD-60 and PD-9, but only reduced persistence for
380 the PD-104. **C)** The use of adjuvant drugs could not prevent persistence. **D)** Combinatorial treatment
381 with amphotericin-B and caspofungin did not prevent persistence. All plates were incubated with 10
382 µL of 0.8 mg/mL voriconazole added to the disc and the specific condition (stress, adjuvant or
383 combinatorial drug) as described in the text. Plates were incubated for 5 days at 37°C. All plates and
384 conditions were repeated in at least two independent experiments.

385

386 **The phenomenon of persistence can be observed with other azole drugs**.

387 To check if *A. fumigatus* can display persistence in the presence of other azoles, we firstly employed
388 the disc diffusion assay adding 10 µL of a 3.2 mg/mL itraconazole solution. We found that the isolates
389 PD-104 and PD-266 were able to form colonies in the halo (Fig. S6). Upon re-inoculation of a CoH (re-
390 grown in itraconazole containing media), the isolate PD-104 showed an inhibition halo of the same
391 size and displayed similar level of CoH appearance, whereas the PD-266 isolate was able to grow on
392 the whole plate and did not show any inhibition halo. Therefore, this suggests that, as observed with
393 voriconazole, the isolate PD-104 is persistent and the isolate PD-266 is heteroresistant to itraconazole.
394 We then performed a broth dilution assay with our four well-characterised isolates (non-persisters
395 ATCC46645 and PD-60 and persisters PD-9 and PD-104) to calculate the MIC for itraconazole and
396 isavuconazole, and looked under the microscope at supra-MIC concentrations (Fig. S7A and S7B). We
397 found that the isolates PD-9 and PD-104 showed slight growth at 2X MIC, whilst ATCC46645 and PD-
398 60 did not (Fig. S7B). Moreover, we inoculated the entire content of wells containing the highest
399 concentration of the drugs (8 µg/mL) on PDA plates, and found that a detectable number of conidia
400 from the isolates PD-9 and PD-104 remained viable after 48 hours of incubation in the presence of the
401 azoles (Fig. S7C). Hence, even if more experiments need to be done for a detailed characterization of
402 persistence to these azoles, these results suggest that the same isolates that are persisters to
403 voriconazole could also display persistence to itraconazole and isavuconazole.

404 **The transcriptome of persister growth suggest that Galactosaminogalactan and high expression of**
405 **sterol biosynthetic genes may be relevant to establish persistence.**

406 To better understand the heterogeneous nature of persistence, we compared the transcriptome of
407 PD-104 grown under conditions favouring persistence (above MIC), sub-MIC and in the absence of
408 drug. We inoculated the spores on top of a nylon membrane placed on an RPMI solid plate. We put
409 the disc with voriconazole (0.8 mg/mL) on the membrane and incubated for 5 days at 37°C. Standard
410 halos of inhibition formed on the membrane, and persister colonies appeared for the PD-104 strain,
411 but not for the A1160 strain (Fig. S8A). We harvested mycelium (avoiding conidia as much as possible)
412 from plates without a voriconazole disc (No Drug), from the area equidistant from the border of the
413 plate and the inhibition halo (Low Drug) and the colonies in the halo (Persistence) (Fig. 4A). We had to

414 combine persister colonies from 20 plates per replicate in order to obtain sufficient material for RNA
415 extraction. Additionally, we harvested mycelia from A1160 with No and Low Drug under the same
416 conditions. We performed RNA-seq of two biological replicates/condition and compared the
417 transcriptomes of the following conditions (i) A1160 Low Drug VS No Drug, (ii) PD-104 Low Drug VS No
418 Drug, (iii) PD-104 Persistence VS No drug and (iv) PD-104 Persistence VS Low Drug. We considered as
419 differentially expressed genes (DEG) those with a log2FoldChange >1 or <-1 and a false discovery rate
420 (FDR) <0.05.

421 In A1160, we detected 62 genes significantly upregulated in the presence of low voriconazole
422 concentrations and only 4 that were downregulated (Fig. 4A and Dataset S1 in
423 https://doi.org/10.5281/zenodo.7021623). Such a low number of DEGs may be due to the relatively
424 low concentration of voriconazole in the harvested area. Nevertheless, among the upregulated genes
425 we found 10 related to sterol biosynthesis (Dataset S1 in https://doi.org/10.5281/zenodo.7021623),
426 including *cyp51A* and *cyp51B*, the expression of which have been reported to increase upon azole
427 challenge [59, 60]. Surprisingly, only 21 of the 62 upregulated genes overlapped with our previously
428 published dataset, in which 1492 genes were upregulated upon challenge of A1160 with itraconazole
429 [61]. This striking difference may be due to the different drug employed, the different concentrations
430 assayed and/or the use of solid medium. Interestingly, these 41 DEGs that are specific to this analysis
431 (which can be found in Dataset S1 in https://doi.org/10.5281/zenodo.7021623) contain *cyp51A*,
432 *cyp51B* and various other genes of the sterol pathway.

433 For PD-104, the Low Drug VS No Drug comparison retrieved 32 genes upregulated and only 1
434 downregulated (Fig. 5 and Dataset S2 in https://doi.org/10.5281/zenodo.7021623). Within the
435 upregulated genes we again found 8 genes related with sterol biosynthesis, including *cyp51A*. In
436 addition, 9 genes did not overlap with the comparison of A1160 (Fig. 4A and Dataset S2 in
437 https://doi.org/10.5281/zenodo.7021623). These differences with A1160 may point to potential
438 strain differences in response to voriconazole. In the Persister VS No Drug comparison there were 802
439 upregulated and 249 downregulated genes and in the Persister VS Low Drug 646 upregulated and 187
440 downregulated genes (Fig. 4A and Dataset S2 in https://doi.org/10.5281/zenodo.7021623). When
441 comparing those three analyses, only 53 genes were exclusively upregulated and 39 downregulated
442 in Persister VS Low Drug (detected using BioVenn [62]), suggesting that they may be important to
443 establish the persister phenotype and not only as a response to the drug (Fig. 4A and Dataset S2 in
444 https://doi.org/10.5281/zenodo.7021623). We performed Gene Ontology (GO) enrichment analyses
445 (on FungiDataBase [63]) for these 53 DEGs, which retrieved a number of biological processes and
446 molecular functions for up- and downregulated genes. It is important to note that the FDR did not
447 reach significance for any of them, which is possibly due to the low number of genes included in the

448 analysis. However, we believe this analysis provided interesting clues and can help to direct future
449 research. For the up-regulated genes, the strongest enrichment was for the biological processes
450 galactose and aldehyde metabolisms (Fig. 4B) and the molecular function oxidoreductase activity
451 (Table S3 in https://doi.org/10.5281/zenodo.7021623). Interestingly, galactose metabolism was
452 found to be the most upregulated function in *Staphylococcus aureus* persisters, although the reason
453 has not been elucidated yet [64]. For the downregulated genes, there was an enrichment of biological
454 processes related with development and cell cycle (Table S3 in
455 https://doi.org/10.5281/zenodo.7021623), possibly reflecting the reduced growth rate in this
456 condition.

457 Interestingly, a significant number of the detected differentially expressed mRNAs in PD-104 were not
458 assigned to any gene of the A1163 genome reference used for the mapping of the reads. In detail, 80
459 of the upregulated (including 4 of the 20 most upregulated) and 29 of the downregulated for the
460 Persister VS no Drug comparison and 55 upregulated (including 5 of the 10 most upregulated) and 14
461 downregulated for the Persister VS no Low comparison seem to have no orthologue in A1163 (Dataset
462 S2 in https://doi.org/10.5281/zenodo.7021623). This points to the requirement of a high number
463 (~10% of the DEG) of strain specific genes to facilitate for persister growth. Therefore, we re-annealed
464 the sequenced mRNAs from the PD-104 isolate to the newly generated *A. fumigatus* pangenome [65]
465 and performed the comparisons again (Dataset S3 in https://doi.org/10.5281/zenodo.7021623). In
466 this analysis, the Persister VS no Drug comparison retrieved 811 genes up- and 260 downregulated,
467 and the Persister VS Low Drug comparison 659 up- and 193 downregulated (Fig. 4A and Dataset S3 in
468 https://doi.org/10.5281/zenodo.7021623). The ratio of identified genes greatly improved, as only
469 ≤1.8% of the DEGs could not be assigned to an ID. Yet, the most upregulated gene in the Persister VS
470 Low Drug comparison was an unidentified gene and many of the newly identified genes encode
471 uncharacterised hypothetical proteins, which reflects our ignorance of *A. fumigatus* biology and thus
472 how difficult it is unravelling underlying mechanisms in this pathogen. GO enrichment analysis of all
473 DEGs showed that secondary metabolism, ergosterol metabolism and transport were key upregulated
474 biological processes (Fig. 4C) and oxidoreductase, catalysis and transmembrane transport important
475 molecular functions (Table S4 in https://doi.org/10.5281/zenodo.7021623), all of which suggests an
476 active metabolic response in persister conditions. As observed above (Table S3 in
477 https://doi.org/10.5281/zenodo.7021623), downregulated biological processes reflected a
478 downregulation of developmental processes (Table S4 in https://doi.org/10.5281/zenodo.7021623).
479 Comparison of the DEGs present in all three comparisons revealed that 64 genes were exclusively up-
480 and 46 downregulated in Persister VS Low Drug (detected using BioVenn [62]), suggesting that they
481 may be specifically important for persistence (Fig. 4A and Dataset S3 in

482 https://doi.org/10.5281/zenodo.7021623). GO enrichment analysis of those genes revealed
483 galactosaminogalactan (GAG) biosynthesis as the most significant upregulated biological process (Fig.
484 4D and Table S5 in https://doi.org/10.5281/zenodo.7021623), providing a plausible explanation for
485 the upregulation of galactose metabolism observed before, and suggesting that this
486 exopolysaccharide may be relevant for persistence in *A. fumigatus*. Next, we performed a protein
487 functional association analysis using the STRING database and platform [66] to investigate if these 64
488 upregulated genes are functionally correlated. Sixty-one of these genes could be matched to proteins
489 in the database, showing a significant ($p$=1.84e-08) interaction network, including a node of 17
490 proteins related with metabolism (Fig. S8B and Table S6 in https://doi.org/10.5281/zenodo.7021623).
491 This suggests that a distinct metabolic response occurs during persister growth.

492

Fig. 4

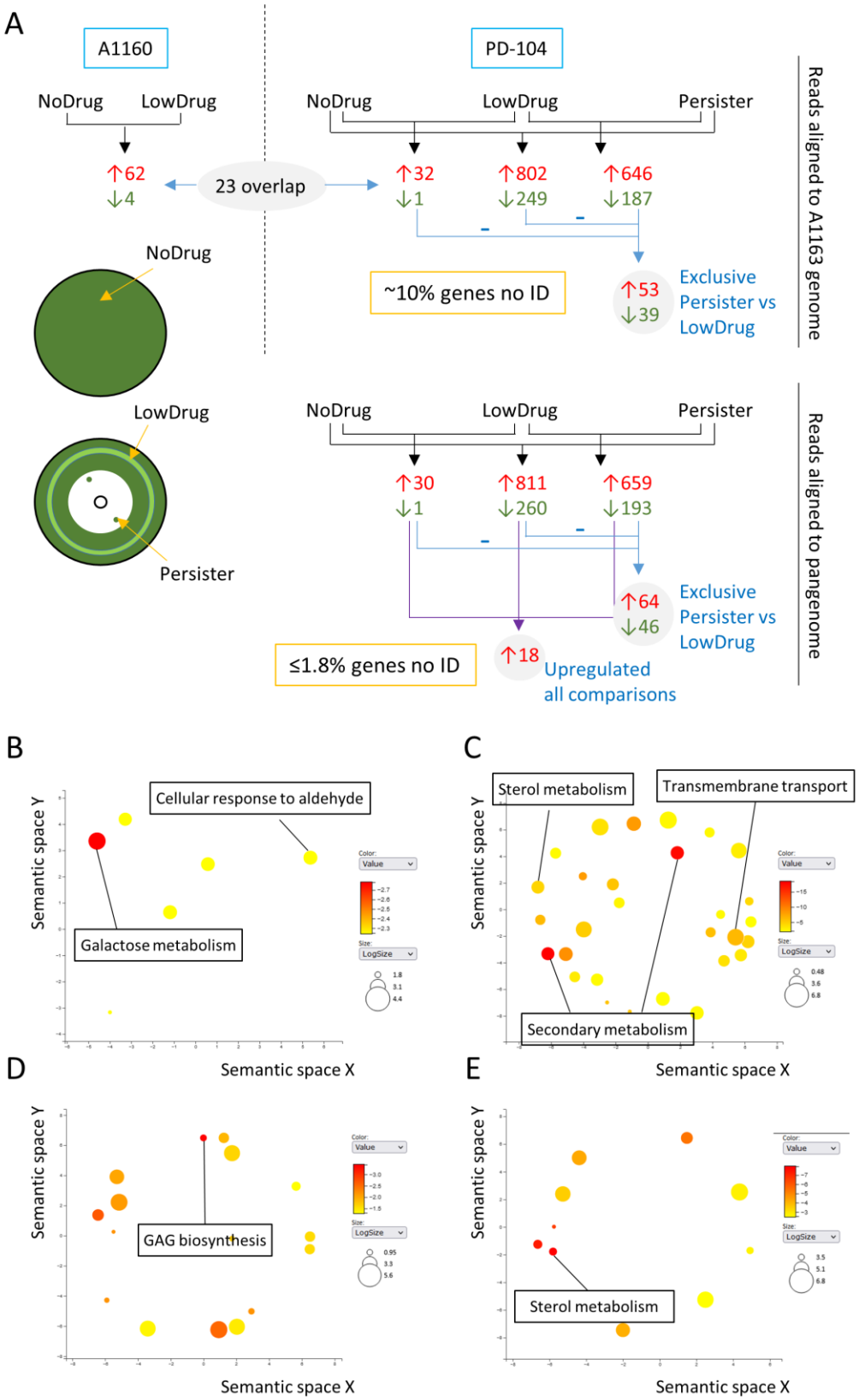


493

494

495

496 **Figure 4. RNA-seq analysis reveals potential causes of persistence**.

497 **A)** Schematic representation of the conditions assayed, the comparisons made and the number of
498 genes identified, as detailed in the text. In addition, the sites of sampling for the no drug (plate without
499 voriconazole disc), low drug (light green circle at mid-distance of the inhibition halo) and persistence
500 (colonies inside the inhibition halos) conditions are shown. **B-E** The most significantly upregulated GO
501 biological processes are shown using the REVINGO tool for GO data visualization [67]. The full list of
502 upregulated GO terms can be found in Tables S2-S5 and Table 3. **B**) PD-104 Persister only genes
503 (aligned to the A1163 genome), **C)** all genes upregulated in Persistence (aligned to the pangenome),
504 **D)** PD-104 Persister only genes, (aligned to the pangenome) and **E)** genes that are most upregulated
505 in persistence compared to normal response to the drug.

506

507 Bacterial persistence has been proposed to be a sub-population event due to stochastic high
508 expression of relevant genes [68, 69]. Accordingly, we reasoned that those genes that are upregulated
509 in Low Drug VS No Drug and Persister VS No Drug comparisons, but also in Persister VS Low Drug might
510 reveal those genes that are important to adapt to presence of the drug, but also that can create
511 persistence with higher levels of expression. We identified 18 genes that appeared as upregulated in
512 all three comparisons (Fig. 4A and Table 3), indicating that they have higher levels of expression in
513 persistence VS normal response to the drug. GO enrichment analysis revealed sterol metabolism as
514 the most significantly upregulated biological process (Fig. 4E and Table S7 in
515 https://doi.org/10.5281/zenodo.7021623). Indeed, those few genes had a very significant enrichment
516 in the KEGG pathway "steroid biosynthesis" (Table 3), suggesting that high expression of genes in the
517 sterol biosynthetic route (including *cyp51A*) may enable the sub-population of persisters to survive
518 and grow in supra-MIC concentrations. Additionally, these highly expressed genes were enriched in
519 KEGG pathways related with cytochrome P450 dependent drug metabolism (Table 3), which may
520 indicate that detoxification of azoles is also important for persistence. Finally, expression of the *cdr1B*
521 transporter (AFUA_1G14330), known to be associated with azole resistance [70], was also detected
522 to be higher in persistence (Table 3). This suggests that a higher capacity to efflux azoles may also be
523 important for the persister phenotype. Finally, we performed a protein functional association analysis
524 with these 18 genes using the STRING database and platform [66] to search for functional correlations.
525 All 18 genes were matched to proteins and a significant interaction ($p$<1.0e-16) was found, involving
526 a highly interactive nodule of 6 proteins related with steroid biosynthesis (Fig. S8C and Table S8 in
527 https://doi.org/10.5281/zenodo.7021623), suggesting again that a high production of ergosterol is
528 important for persistence.

529

530

531

| Gene ID | Product description |
|---|---|
| AFUA_1G03200 | Putative major facilitator superfamily (MFS) transporter |
| AFUA_4G06890 | 14-alpha sterol demethylase Cyp51A |
| AFUA_2G00320 | putative sterol delta 5,6-desaturase |
| AFUA_3G00810 | Putative cholestenol delta-isomerase |
| AFUA_1G03150 | C-14 sterol reductase, putative |
| AFUA_8G02440 | C-4 methyl sterol oxidase, putative |
| AFUA_6G14140 | Has domain(s) with predicted role in response to stress and integral component of membrane localization |
| AFUA_3G00150 | Has domain(s) with predicted oxidoreductase activity and role in metabolic process |
| AFUA_4G01440 | Predicted glutathione S transferase |
| AFUA_4G04820 | C-4 methyl sterol oxidase Erg25, putative |
| AFUA_5G00840 | Ortholog of *A. nidulans* FGSC A4 : AN5639, AN2587, AN9444, AN7395, |
| AFUA_2G15130 | ABC multidrug transporter A-2, putative |
| AFUA_5G03290 | Ortholog of *A. nidulans* FGSC A4 : AN8197, A |
| AFUA_3G02520 | Has domain(s) with predicted role in transmembrane transport and integral component of membrane localization |
| AFUA_7G04740 | Ortholog of *A. fumigatus* Af293 : Afu1g01960, Afu3g01040, Afu3g03315, Afu7g01960, Afu8g05750, Afu5g00135, Afu7g06526 |
| AFUA_2G01890 | Ortholog(s) have 2-octoprenyl-3-methyl-6-methoxy-1,4-benzoquinone hydroxylase activity, |
| AFUA_1G14330 | Azole transporter |
| AFUA_8G00710 | Has domain(s) with predicted role in defense response, negative regulation of growth |

| KEGG Pathway | | | |
|---|---|---|---|
| ID | Name | P-value | Benjamini |
| ec00100__PK__KEGG | Steroid biosynthesis | 2,31E-08 | 1,18E-06 |
| ec00980__PK__KEGG | Metabolism of xenobiotics by cytochrome P450 | 0.002873 | 0.07326 |
| c00982__PK__KEGG | Drug metabolism - cytochrome P450 | 0.004423 | 0.07520 |

532 **Table 3**. GO biological processes enrichment and KEGG pathway enrichment for the 18 genes that
533 showed higher expression in Persistence than in NoDrug and LowDrug.

534

535 **Galactosaminogalactan potentiates persistence of PD-104.**

536 Our transcriptome analysis detected a significantly higher expression of two GAG biosynthetic genes
537 (*sph3*, AFUA_3G07900 and *uge3*, AFUA_3G07910) in persister growth (Dataset S3 in
538 https://doi.org/10.5281/zenodo.7021623). Manual inspection of the GAG biosynthetic genes [71, 72]
539 revealed that another gene (*agd3*, AFUA_3G07870) might also be upregulated (FC= 1.01), but
540 although the *p*-value was significant (*p*= 0.0179), the FDR rate was above threshold (FDR=0.1167)
541 (Dataset S3 in https://doi.org/10.5281/zenodo.7021623). This prompted us to investigate if a higher

542 amount of GAG could create and/or potentiate persistence in *A. fumigatus*. To this aim, we performed
543 broth dilution assays in which we inoculated each isolate (ATCC, PD-9, PD-60 and PD-104) in two
544 different lines and added purified GAG at a concentration of 100 µg/mL to one of them. Comparison
545 of the MIC with and without GAG demonstrated that this polysaccharide did not affect the resistance
546 profile of the isolates (Fig. 5A). After reading the MIC at 48 hours, we added 10 µg/mL of the dye
547 calcofluor white (CFW) to the wells and imaged the entire well (87 photos using a 20X objective) at
548 the blue emission channel. Images were merged (Fig. 5B) and the number of germinated conidia/short
549 hyphae in the whole well calculated as explained in materials and methods (Fig. 5B). By these means
550 we could calculate that ~2% of the PD-9 spore population and ~1% of the PD-104 conidia were able to
551 germinate at 2X MIC, and ~0.35% for both isolates in 3X MIC. Interestingly, addition of GAG enhanced
552 the number of persisters in PD-104 (from 1.09% to 2.80%, $p$=0.0267 at 2X MIC and from 0.41% to
553 0.75% $p$=0.038) but not in PD-9 (Fig. 5B). Next, we inoculated the four isolates in duplicated lines of
554 96-well plates containing a high concentration of voriconazole (4 µg/mL) in all wells, and added GAG
555 to one line of each isolate. The entire contents of wells were plated 48 hours after inoculation on PDA
556 rich plates to count the number of viable CFUs. As observed before (Fig. 1C), we found that the
557 persister isolates (PD-9 and PD-104) maintained viability of a significant number of conidia for an
558 extended period of time (Fig. 5C). Interestingly, GAG addition seemed to slightly increase the number
559 of grown CFUs for all isolates, although this increment was only significant for the PD-104 isolate (PD-
560 104 VS PD-104+GAG $p$=0.0437).

561 These results suggest that a high level of GAG can potentiate persistence in some, but apparently not
562 all, isolates. Future investigations will aim to understand the underlying mechanism and to determine
563 why GAG addition is isolate-specific.

Fig. 5

A

| Voriconazole | | |
|---|---|---|
| Isolate | MIC | MIC +GAG |
| ATCC | 0.5-1 | 0.5-1 |
| PD-9 | 0.5-1 | 0.5-1 |
| PD-104 | 0.5-1 | 0.5-1 |
| PD-60 | 0.5-1 | 0.5-1 |

B

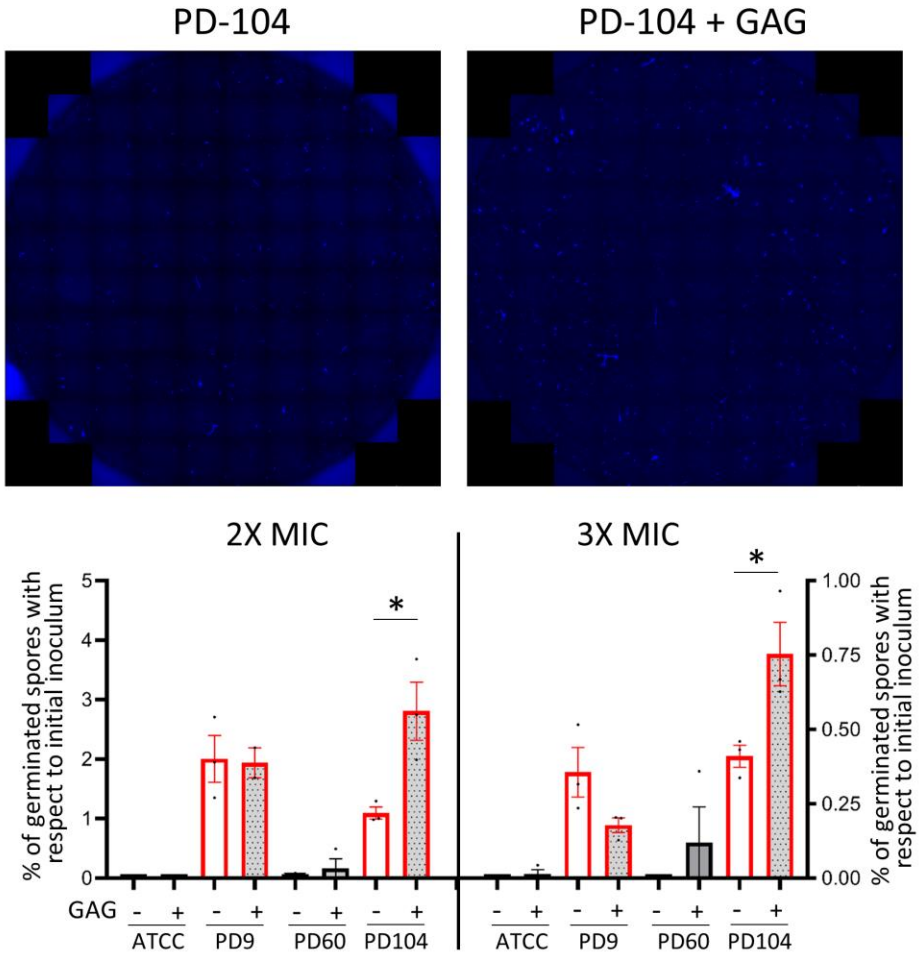


C

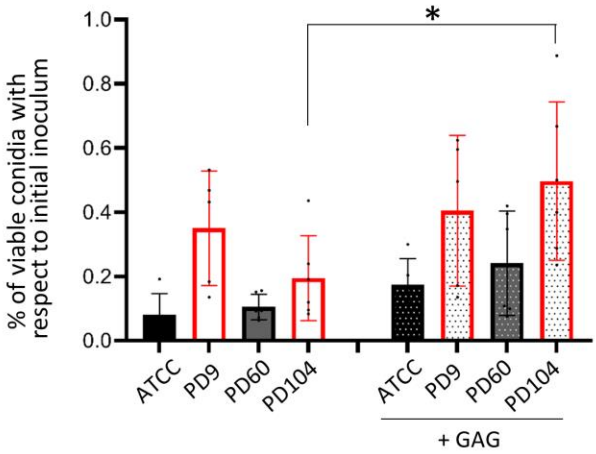


564

565

566 **Figure 5. External addition of GAG potentiates persistence in the isolate PD-104**.

567 **A)** Addition of GAG does not change the MIC of the isolates. **B)** Representative merges of 87 photos
568 to cover the whole well of broth dilution assays. The fungal material was stained with calcofluor white.
569 Representative wells of PD-104 with and without GAG at 2X the MIC are shown **C)** Counting of
570 germinated conidia/short hyphae in the entire wells of 2X (left) and 3X (right) MIC of broth dilution
571 assays. External addition of GAG significantly increased the number of germlings in PD-104 from 1.09%
572 to 2.80%, $p$=0.0267 at 2X MIC and from 0.41% to 0.75% $p$=0.038, two-tailed unpaired $t$-test. Two
573 independent experiments with three technical replicates were performed. The graphs represent the
574 means and SD. **D)** Plating of the entire content of wells containing 4 µg/mL of voriconazole shows that
575 external addition of GAG significantly increased the number of viable PD-104 cells that can be
576 recovered 48 hours after inoculation ($p$=0.0437, one way ANOVA with Tukey's multiple comparisons).
577 Two independent experiments with three biological replicates were performed. The graph represents
578 the means and SD.

579

580 **Persistence can be detected in diverse *A. fumigatus* collections of isolates**

581 To corroborate that certain *A. fumigatus* isolates display persistence to voriconazole, we decided to
582 screen two independent collection of isolates. Initially, we tested an environmental library of isolates
583 collected in the area of Manchester, UK [73]. We screened all 157 isolates for growth under the
584 microscope after 72 hours incubation in the presence of a high concentration of voriconazole (8
585 µg/mL). We found that 34 isolates were able to show a limited degree of growth, suggesting that they
586 might be persisters (Table S9 in https://doi.org/10.5281/zenodo.7021623). Next, we employed disc
587 diffusion assays with 0.8 mg/mL voriconazole and observed that 15 out of the 34 isolates were able to
588 form colonies in the halo (Table S9 in https://doi.org/10.5281/zenodo.7021623). Broth dilution assay
589 with the original isolates and the CoHs revealed that 10 of those isolates did not have increased MICs,
590 indicating that they were persister strains (Table S9 in https://doi.org/10.5281/zenodo.7021623).
591 Therefore, at least ~6% of this collection was persister to voriconazole. We further evaluated a
592 collection of 17 azole-susceptible clinical isolates obtained from TAU medical centre (Table S9 in
593 https://doi.org/10.5281/zenodo.7021623), which were prior shown not to have any mutation in the
594 *cyp51A* gene promoter or ORF, using the disc diffusion assay. We found that 6 out of 17 (35%) isolates
595 were able to grow small colonies in the inhibition halo (Fig. S9A). Colonies picked from within the halo
596 formed upon re-inoculation similar size halos, indicating that the MIC had not increased, and grew a
597 similar number of CoHs, suggesting that the isolates are persisters.

598 Therefore, evaluation of independent collection of isolates seem to always retrieve a significant
599 number of persister strains, demonstrating that this is quite a common phenomenon.

600 **Persistence is not a lineage specific trait.**

601 Recent studies suggest that the tandem repeats (TRs) in the promoter region of *cyp51A*, which cause
602 high levels of antifungal resistance, possibly have evolved in the environment, due to the use of

603 demethylase inhibitors (azoles) in the fields [74]. Interestingly, the isolates with the $TR_{34}$/L98H
604 polymorphism have been found to be closely related [65, 74], which suggest that this mechanisms has
605 evolved in a distinct lineage of the species. To investigate if the phenomenon of persistence could also
606 be lineage specific, we sequenced the genome of 23 of our isolates, 12 persisters and 11 non-persisters
607 (Table S9 in https://doi.org/10.5281/zenodo.7021623) and integrated their genome into a recently
608 published phylogenetic analysis [65]. We found that both persister and non-persister isolates
609 scattered through the entire tree, demonstrating that persistence is not a trait of a specific lineage of
610 *A. fumigatus* (Fig. 6). In addition, it is noteworthy that some persister and non-persister isolates seem
611 to be genetically very similar, as they are close in the tree (JA12-JA14-JA7-JA8 and also JA1-JA2, Fig.
612 6). This suggests that the genetic features that enable persistence are modest and/or that non-
613 genomic features, as the transcriptional response, are important for isolate specificity.

Fig. 6

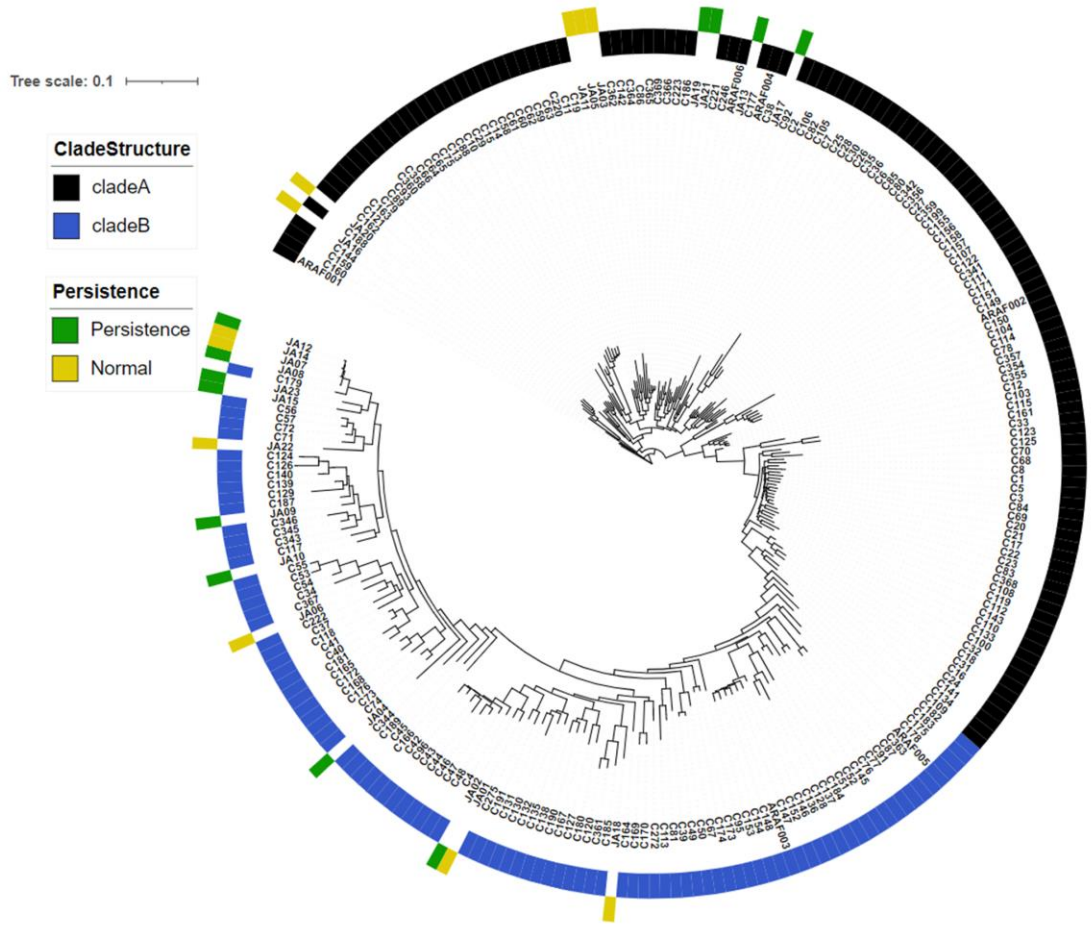


614

615 **Figure 6. Persister isolates do not form a distinct lineage.**

616 The genomes of newly sequenced persister and non-persister isolates, as characterised in this study
617 (Table S9 in https://doi.org/10.5281/zenodo.7021623), distributed scattered when included in the

618 previously generated phylogenetic tree [65]. Therefore, persistence is not a feature that has evolved
619 in a particular lineage.

620 **In a *Galleria mellonella* infection model, a voriconazole treatment seems to be less efficient against**
621 **persister isolates in some larvae.**

622 To evaluate if persistence may be relevant during antifungal treatment, we employed the *Galleria*
623 *mellonella* mini-host model of infection. This model has been successfully used to investigate the
624 efficiency of azole treatment against *A. fumigatus* [75, 76]. In addition, a recent study has
625 characterised the pharmacokinetics of voriconazole in infected larvae, which allowed us selecting the
626 optimal dose to reach a high concentration of the drug in the haemolymph (above the MICs of the
627 isolates), but that is nearly completely removed in 24 hours [77].

628 Initially, we performed a survival experiment with all four strains to investigate if they could have
629 different virulence potential. We infected larvae with $10^4$ or $5\times10^4$ conidia of non-persister
630 (ATCC46645 or PD-60) or persister (PD-9 or PD-104) isolates and followed mortality for 10 days. All
631 the isolates killed larvae at a similar rate (Fig. S9B), demonstrating that they are similarly virulent.
632 Therefore, we aimed to use this model to investigate if persistence could potentially cause treatment
633 failure. We reasoned that a voriconazole treatment should very efficiently eradicate susceptible, non-
634 persister strains, but it may not be able to eliminate persister strains with the same efficiency in all
635 individuals. We infected larvae with $10^4$ (Fig. 7A) or $5\times10^4$ (Fig. 7B) conidia of non-persister
636 (ATCC46645 or PD-60) or persister (PD-9 or PD-104) isolates, administered one dose of 8 µg/larva
637 voriconazole or PBS at the time of infection, and measured fungal burden 72 hours (Fig. 7A) or 48
638 hours (Fig. 7B) after infection. As expected, voriconazole treatment was efficient and dramatically
639 decreased fungal burden for all isolates (Fig. 7A and B). To note, for voriconazole treated groups, the
640 mean of fungal burden was bigger for persisters than for non-persister isolates, although these
641 differences were not significant (ATCC VS PD-9 $p$=0.41 for $10^4$ and $p$=0.57 for $5\times10^4$, ATCC VS PD-104
642 $p$=0.27 for $10^4$ and $p$=0.69 for $5\times10^4$, Mann-Whitney test), due to the high variability in burden among
643 individuals infected with the persister isolates. Indeed, at both infectious doses several larvae infected
644 with persister isolates had noticeable greater burdens than all the other (Fig. 7A and B), which we
645 speculate might indicate that in some individuals infected with persistent isolates treatment may be
646 less efficient in eliminating the fungus.

647

Fig. 7

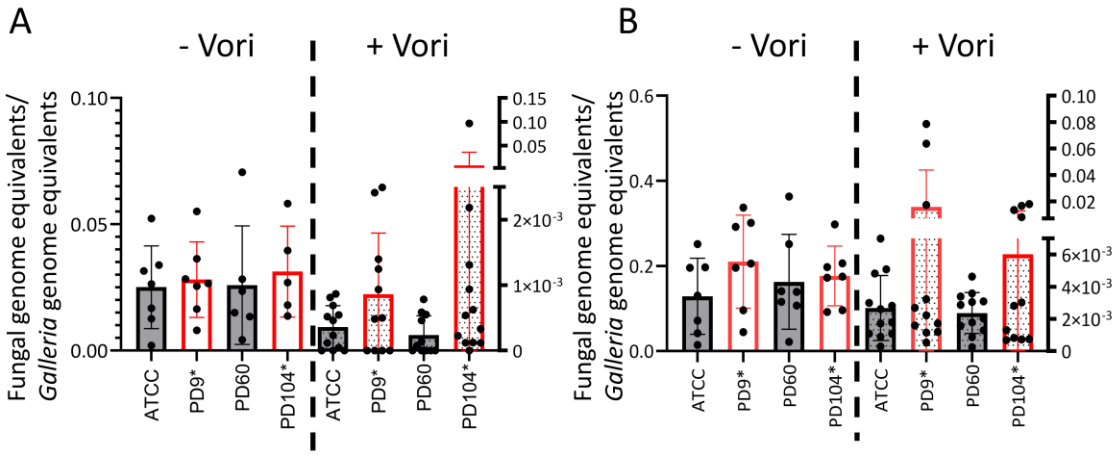


**Figure 7. In some larvae, voriconazole eliminates persister isolates less efficiently than non-persister strains in a *Galleria mellonella* infection model.**

Fungal burden was measured by qPCR **A)** 72 h after infection with $10^4$ conidia, or at **B)** 48 h after infection with $5\times10^4$ conidia For all strains, fungal burden was greatly lower in larvae that had received a voriconazole treatment (8 µg/mL) that in those who had not. The reduction in burden was bigger in non-persister isolates than in persister isolates, although these differences were not significant. Several treated larvae infected with persister isolates had noticeable higher burdens than the other: **A)** 4/11 for PD-9 and 3/11 for PD-104 **B)** 3/11 for PD-9 and 4/11 for PD-104. Each graph displays the combined data from two independent experiments.

## DISCUSSION

The phenomenon of persistence to antimicrobials was first observed in bacteria 80 years ago [78, 79]. In the last decade, intensive research has permitted unravelling various underlying mechanisms in diverse bacteria, and it has become clear that persistence can cause treatment failure and lead to the development of resistance [80, 81]. However, our insight into antifungal persistence and tolerance in fungal pathogens is still in its infancy.

We have recently shown that all conidia in a tolerant *A. fumigatus* isolate are able to grow at high concentrations of caspofungin [26]. In *C. albicans*, tolerance to fluconazole was described to be a sub-population effect, but the ratio of tolerant cells was reported to be elevated [21]. In both cases, tolerance was observed in response to static drugs, so it seems that the phenomenon of tolerance in fungi associates with fungistatic drugs. In *C. albicans*, the formation of amphotericin-B (AmB) persister cells has been described [82]. Of note, this phenomenon has only been described within biofilms, and cannot be found in planktonic cells [83], possibly due to the physical protection conferred by the biofilm, which may be relevant for the capacity of these cells to survive in the presence of AmB. Indeed, in *A. fumigatus* it was shown that the hypoxic microenvironment developed in biofilms led to

674 reduced metabolic activity in the basal biofilm level leading to the formation of cells that can survive
675 the antifungal challenge, and serve as a drug-resistant reservoir [84].

676 We have observed that a small sub-population (0.1 to 5%) of certain *A. fumigatus* isolates can survive
677 for extended periods and even grow at slow rates in the presence of supra-MIC concentrations of the
678 fungicidal drug voriconazole. In bacteria, tolerance and persistence have been classically explained by
679 a downregulation of metabolism and cell cycle, which trigger a status of dormancy that permit survival
680 despite the action of the drug. However, recent research in pathogenic bacteria has demonstrated
681 that active metabolic responses are required for persistence [85, 86], and slow-growing persisters
682 have also been detected *in vitro* [87] and *in vivo* [88]. Active metabolism may even be advantageous,
683 as in the case of *Salmonella*, where persisters have been shown to undermine host defences [89].
684 Interestingly, *C. albicans* AmB persistence has been described to involve downregulation of primary
685 metabolism, but also an increase of stress responses and oxidative defensive mechanisms [90]. We
686 have observed that active growth is possible at two or even three-fold the MIC, and that this growth
687 entails a distinct transcriptional profile. Therefore, this phenomenon is not merely survival of dormant
688 conidia in the presence of the drug, but seems to be an active mechanism that enables a sub-
689 population of certain isolates to withstand the action of voriconazole for an extended period. Indeed,
690 using resazurin (an oxidation-reduction indicator used for the measurement of metabolic activity and
691 proliferation of living cells, which use has been optimised for *A. fumigatus* [91]) we could detect a
692 slight metabolic activity at supra-MIC concentrations (Fig. S9C). This might explain why hypoxia is the
693 only environmental condition that reduced persistence, as in low oxygen the metabolic activity is
694 reduced [84] and the energy generating metabolism changes [92].

695 We have observed a big difference in growth between liquid media (only microscopic growth) and
696 solid media (macroscopic colonies). We hypothesise that this may be because in agar drug
697 microdepletions around the hyphae would diffuse back much slower than in liquid, giving an
698 advantage to the hyphae in solid media. In addition, there may be a different level of contact of
699 conidia with the drug; in liquid, the conidia are completely surrounded, whilst on solid media the
700 conidia just lay on the drug and may escape from it by orientating the germling polarity as they grow.

701 It is surprising that we have not found any voriconazole tolerant isolate. It might be that the frequency
702 of this phenomenon is lower in *A. fumigatus* (even in filamentous fungi in general), and we simply
703 have not screened enough isolates to detect it. However, we believe that the particularities of working
704 with filamentous fungi make the definitions developed with bacteria unsuitable. Firstly, MIC
705 measurements or killing curves need to be done over a period of days, compared with hours for
706 bacteria. In addition, the inoculum used is normally conidia, a dormant cell structure that needs to be

707 activated to produce an effect. Besides, the experiments are performed with inocula of around $10^4$
708 ($2.5\times10^4$ for broth dilution and $4\times10^4$ for disc assays) conidia, whilst bacteria persistence can be
709 assayed with inocula in the range of $10^6$ – $10^8$ cells. Therefore, we believe it would be challenging to
710 clearly discern between the duration of killing for 99% or 99.99% of the cells, the most important
711 factor to differentiate tolerance and persistence [18, 19]. Indeed, looking closely at the killing curve
712 presented in Fig. 1D, at 2 days the percentage of survivors is 99.38% for PD-9 and 99.86% for PD-104.
713 Could this mean that PD-9 is tolerant and PD-104 a persister? This seems to be supported by the
714 experiments plating wells from the broth dilution assays (Fig. 1C and 5C), where more colonies are
715 counted for PD-9 than for PD-104. However, the number of colonies detected in the disc assays is
716 usually higher for PD-104 (2-5) than for PD-9 (1-2). Given that the mechanisms of tolerance and
717 persistence in bacteria are multiple and overlapping [93], we propose to define the phenomenon that
718 we have described in this study as persistence and utilize the term tolerance to define the effect
719 previously described with fungistatic drugs [21, 26]. Therefore, we propose to adapt the current
720 definitions for pathogenic fungi as presented in Table 1.

721 The concept of persistence entails two intriguing aspects. Firstly, it is an isolate-dependent
722 phenomenon, which means that there must be a genetic basis that underlies persistence. We have
723 shown that the persister isolates do not belong to a specific lineage, suggesting that this feature has
724 not appeared as an evolutionary trait in a lineage of isolates. Recently, it has been described that each
725 *A. fumigatus* strain carries a particular set of accessory genes, which associates with different levels
726 of virulence and drug resistance capacities [94]. In the same vein, we speculate that the presence or
727 absence of certain accessory genes may enable certain isolates to persist in the presence of azoles.
728 Future research will evaluate if this hypothesis is true. A second intriguing aspect of persistence is that
729 it is a sub-population phenomenon, meaning that within an isogenic isolate only a few conidia are able
730 to survive and grow in the presence of the drug. In bacteria, stochastic expression of key genes has
731 often been proposed as an important underlying cause of persistence [68, 69, 95, 96]. This includes
732 stochastic high expression of genes that directly confer resistance [97] and efflux activity [98].
733 Similarly, in our RNA-seq analysis we have detected a higher level of expression of genes of the sterol
734 biosynthesis pathway, including *cyp51A*, and of the azole exporter Cdr1B in persister cells. Therefore,
735 it is plausible that stochastic high levels of these genes could generate the capacity to survive for an
736 extended period in the presence of supra-MIC concentrations of voriconazole. Additionally, we
737 detected a higher level of expression of GAG biosynthetic genes, and we have observed that externally
738 added GAG can increase the number of persisters in the isolate PD-104. Interestingly, this
739 polysaccharide did not increase the isolate's MIC, indicating that it does not provide a physical barrier
740 that shields the fungus or that it cannot somehow degrade the drug. Future investigations will aim to

741 unravel why GAG potentiates persistence in PD-104, and not in PD-9, which is interesting as it suggests
742 that there might be multiple persistence mechanisms. GAG is a very relevant *A. fumigatus* virulence
743 factor, with multiple described adhesion and immunosuppressive activities [99, 100], and here we
744 propose that it may have one more important role in potentiating persistence to voriconazole.

745 In bacterial infections, there is significant evidence supporting a role for the phenomena of tolerance
746 and persistence in antibiotic treatment failure [16, 101]. In contrast, the knowledge about these
747 phenomena in fungal infections is still very scarce. Probably, the best-studied phenomenon is
748 heteroresistance in *Cryptococcus neoformans* and *C. gatii* [102-104], which has been found to be a
749 major cause of treatment failure in cryptococcal meningitis [105-109]. As mentioned above, there is
750 already evidence indicating that fluconazole tolerance can cause treatment failure in invasive
751 candidiasis [17, 21], and limited evidence suggests that caspofungin tolerance may cause treatment
752 failure in *Aspergillus* infections [27]. Here, using a *Galleria* model of infection, we have observed that
753 voriconazole treatment seems to eliminate persister isolates less efficiently than non-persister isolates
754 in various larvae. Therefore, we hypothesise that in certain individuals persistence might reduce the
755 efficacy of voriconazole treatment in *A. fumigatus* infections, which, if proven true, could imply that
756 persistence may cause therapeutic failure in some patients. In addition to such a potential direct effect
757 of persistence on treatment failure, resilience and relapse of persistent strains could associate with
758 the development of antifungal resistance (an effect that has already been shown for bacterial
759 infections, see [110] for references), as it is known that prolonged azole treatment can result in
760 resistance [111, 112]. We appreciate that our results provide limited evidence to support the
761 hypothesis that voriconazole persistence may cause treatment failure, and acknowledge that much
762 more research is required to reach such conclusion. We will continue investigating this hypothesis and
763 we exhort the fungal research community to consider and investigate this phenomenon to clarify this
764 important matter.

765

766 **MATERIAL and METHODS**

767 ***A. fumigatus* strains and culture conditions.**

768 All isolates utilized in the course of this study are listed in Tables S1 and S8. Briefly, information about
769 the common laboratory strains used can be found in [113], the isolates from Paul Dyer collection are
770 described in [114] and the collection of isolates from the area of Manchester are described in [73].
771 The third collection of isolates was collected at the TAU medical centre (Tel-Aviv, Israel), these strains
772 were characterized for their antifungal resistance profile and *cyp51A* genotype. Persister isolates are
773 labelled in all figures with an asterisk (*).

774 Isolates were routinely grown on Potato Dextrose Agar (PDA, Oxoid) for 72 hours to obtain fresh
775 spores for each experiment. All experiments were performed with fresh spores except in the test for
776 persistence with old conidia. *Aspergillus* Minimal Medium (AMM) was prepared following a standard
777 recipe [115]. Sabouraud (Oxoid) and yeast extract glucose (YAG, 2%, 0.5% yeast extract, 1.7% agar, 1X
778 trace elements) media were used in specific experiments.

779 To evaluate persister growth and determine the MIC, isolates were grown on RPMI-1640 (Sigma) with
780 35 g/L MOPS (Alfa Aesar) and 2% glucose, pH 7.

781 Galactosaminogalactan (GAG) was obtained from the *A. fumigatus* Δ*ku80* strain, grown 2-day in 1.5L
782 brian fermenter at room temperature. GAG isolation and purification was carried out as previously
783 described [116]. Briefly, the medium supernatant was collected by filtration and was adjusted to pH 3
784 by addition of 100 µl 12 M HCl per 100 ml supernatant. Two volumes of precooled ethanol (4°C) were
785 added and GAG was precipitated for 3 h at 4°C. The precipitate was collected by centrifugation for 20
786 min at 5,000 g at 4°C and subsequently washed twice with 1/10 of the culture volume of 200 mM NaCl
787 for 1 h under agitation (100 rpm). GAG was dialyzed against tap water and twice against purified water
788 (24 h each) and finally lyophilized to dryness and stored at ambient temperature.

789 To calculate germination rate, $10^4$ conidia of each strain were inoculated in 200 µL liquid RPMI in 96-
790 well plates and imaged a Nikon TI microscope equipped with a 37 °C incubator and a 40× objective,
791 with 1 picture captured every 30 min by using NIS-Elements 4.0 (Nikon) software. Cell Counter plug-
792 in of Image J platform (http://rsb.info.nih.gov/ij/index.html) was employed to differentially count
793 resting or swollen conidia versus germinated conidia.

794 To calculate growth rate on solid medium, $10^3$ conidia of each strain were inoculated on RPMI plates,
795 and the colony diameter was measured in two different angles per colony at 16, 24, 40 and 48 h. To
796 calculate growth rate on liquid medium $2\times10^3$ of each strain were inoculated in 200 µL liquid RPMI in
797 96-well plates and optical density measurements were taken at 600 nm every 10 minutes. Growth
798 curves were analysed using the R package Bayesian Estimation of Change-points in the Slope of
799 Multivariate Time-Series (BEAST) [117] With parameters; burn = 2000, 5000 iterations,
800 zeroNormalization=TRUE and a blankThreshold of 0.095. Confidence intervals of the first change-point
801 were plotted in Graphpad PRISM.

802 **Evaluation of persistence and determination of MICs**.

803 To determine persistence using the disc assay, $4\times10^4$ conidia of each isolate was evenly spread on a
804 solidified RPMI plate (1.5% agar) and 10 µl of 0.8 mg/mL voriconazole or 3.2 mg/mL itraconazole
805 (Acros Organics) was added to a Whatman 6 mm antibiotic assay disc which was placed in the middle
806 of the plate. For *in vitro* treatment with adjuvant and combinatorial drugs, the agents were added to

807 the RPMI medium at the final concentration detailed in each section. Plates were incubated for 5 days
808 at 37 °C. Persister colonies were defined as those with a degree of physical separation from the edge
809 of the loan of growth into the halo of inhibition.

810 Minimum inhibitory concentrations (MICs) were calculated using the broth microdilution method
811 according to the EUCAST E.Def. 9.3 instructions [118]. $2.5\times10^4$ conidia were used in each well.

812 **Evaluation of the conidial survival to voriconazole fungicidal action**

813 To calculate the number of conidia that survived after exposure to high concentration of azoles, full
814 contents of the wells containing the highest concentration of each drug (8 µg/mL) in the broth dilution
815 assays were plated after 48-72 hours incubation on PDA and further incubated for 24-48 h at 37 °C.

816 Microscopic analysis was used to investigate the survival of strains upon withdrawal of voriconazole
817 at single cell level. $1.5\times10^4$ conidia of each strain were inoculated in 300 µL of RPMI in the presence of
818 8 µg/mL voriconazole (European Pharmacopoeia, -EP- Reference Standard, Merck) and incubated for
819 48 hours at 37 °C with occasional shaking. The strains were then centrifuged for 4000 RPM for 5
820 minutes, the media discarded and the conidia resuspended in 2 mL filtered PBS. This wash was
821 repeated three times in total before the conidia were resuspended in 600 µL of drug free RPMI. 300
822 µL of each suspension, approximately $7.5\times10^3$ conidia, was added into wells of a 96 well plate. The
823 wells were then imaged for 72 hours, every 2 hours, on a Nikon Eclipse Ti microscope, using a Nikon
824 CFI Plan Fluor ELWD 20x/0.45na objective, and captured with a Hamamatsu ORCA-FLASH4.0 LT+
825 camera (Hamamatsu Photonics) and manipulated using NIS-Elements AR 5.11.01 (Nikon). A video was
826 prepared using Fiji [119].

827 Microscopy to observe growth at supra-MIC conditions was done in a THUNDER Imager Live Cell
828 microscope, with a HC PL FLUOTAR L 20x/0.40 DRY objective. Images were captured using a Leica-
829 DFC9000GTC-VSC13067 camera and the Las X (Leica application suite) v 3.7 software.

830 To construct the killing curved, the isolates were inoculated in 10 mL of RPMI containing 4 µg/mL
831 voriconazole. Aliquots for each culture were taken at the time of inoculation (100 µL) and every 24
832 hours (1 mL). The aliquots were spun at 16,000 ×g for 5 minutes, resupended in 1 mL PBS and vortexed.
833 This was repeated twice to wash off the drug. Finally, conidia were resuspended in 1 mL PBS and a
834 fraction plated on PDA plates (50 µL at time 0h, 100 µL at 24h and 1 mL for 48, 72 and 96 h). The
835 experiment was repeated three times.

836 To calculate the percentage of germinating conidia, the wells of broth dilution assays containing 2X,
837 3X MIC and the maximum drug concentration (8 µg/mL) were stained (after reading the MIC) with 10
838 µg/mL of Calcofluor White (Sigma) for 5 minutes. The entire wells were imaged with a THUNDER

839 Imager Live Cell microscope, using a HC PL FLUOTAR L 20x/0.40 DRY objective, filter conditions:
840 EX:375-435 DCC:455 EM:450-490, a Leica-DFC9000GTC-VSC13067 camera and the Las X (Leica
841 application suite) v 3.7 software. Merged images were analysed using FIJI [119]. Briefly, the merged
842 images were converted to 8-bit, a threshold was set for the images so that the conidia and germlings
843 could be detected over the background (20 to 255). The option analyse particle was then executed,
844 setting a minimum size of 0.04 inches$^2$ (which was found to exclude resting conidia). Wells containing
845 the maximum concentration of the drug, where only resting conidia can be found, were used to set
846 the background level of detection for each isolate (consisting of aggregates of conidia, impurities and
847 carry over conidiophores from the inoculum). The percentage of germinated conidia/short hyphae
848 was calculated as: (number of counted particles per well – number of counted particles in max
849 drug)/25000 (inoculum).

850 **Nucleic acid isolation**

851 For DNA extraction, $10^6$ spores of each *A. fumigatus* isolate were grown overnight on liquid *Aspergillus*
852 minimal medium, filtered through Miracloth paper (Merck), snap frozen and ground in constant
853 presence of liquid nitrogen. Subsequently, DNA was extracted using a standard CTAB method.

854 For RNA extraction, *A. fumigatus* isolates were grown on 0.45 µm pore nylon membranes (GE
855 Healthcare) placed on RPMI plates and incubated 1 day (without drug) or 5 days (with voriconazole in
856 a disc). Mycelia were scratched using a spatula and immediately frozen and grounded in liquid
857 nitrogen. Subsequently, RNA was extracted and purified with the Plant RNeasy Mini Kit (Qiagen)
858 following the manufacturer's instructions for filamentous fungi, and using on-column DNase
859 treatment.

860 For fungal burden calculations in *Galleria mellonella*, DNA was extracted from decapitated larvae using
861 the DNeasy Blood & Tissue Kit (Qiagen) following the manufacturer's instruction for animal tissue,
862 with overnight incubation at 56 °C.

863 ***Galleria mellonella* infection**

864 Sixth-stage instar larval *G. mellonella* moths were purchased from R.J.Mous Livebait (Eigen Haard, The
865 Netherlands). Randomly selected groups of 250-350 mg of weight larvae were injected in the last left
866 proleg with 5 µL of a $2\times10^6$ conidia/mL suspension ($10^4$ conidia/larva) of the correspondent *Aspergillus*
867 *fumigatus* isolate using Hamilton syringe. 2 hours after infection, relevant groups were injected in the
868 last right proleg with 5 µL of a suspension containing 1600 µg/mL (8 µg/larvae) voriconazole. A PBS
869 control group was subjected to the same treatment, but without fungal infection.

870 To detect the fungal burden, 500-ng portions of DNA extracted from each larva were subjected to
871 qPCR using the SensiMic SybR Green kit (Bioline). Forward (5'-ACTTCCGCAATGGACGTTAC-3') and
872 reverse (5'-GGATGTTGTTGGGAATCCAC-3') primers were used to amplify the *A. fumigatus* β-tubulin
873 gene (AFUA_7G00250). The primers designed to amplify the Elongation factor 1-Alpha (Ef-1a) were as
874 follows: forward (5'- AACCTCCTTACAGTGAATCC-3') and reverse (5'- ATGTTATCTCCGTGCCAG-3').
875 Standard curves were calculated using different concentrations of fungal and larval gDNA pure
876 template. Negative controls containing no template DNA were subjected to the same procedure to
877 exclude or detect any possible contamination. Three technical replicates were prepared for each
878 sample. qPCRs were performed using a CFX96 Real-Time System (Bio-rad) with the following thermal
879 cycling parameters: 95°C for 10 min and 40 cycles of 95°C for 15 s and 58°C for 15 s and 72°C for 15 s.
880 The fungal burden was calculated by normalizing the number of fungal genome equivalents (i.e., the
881 number of copies of the tubulin gene) to the larval genome equivalents in the sample (i.e., the number
882 of copies of the a Ef-1a gene), as we have reported before [120].

883 **RNA sequencing (RNA-seq)**

884 Total RNA was submitted to the Genomic Technologies Core Facility (GTCF) at the University of
885 Manchester, UK. Quality and integrity of the RNA samples were assessed using a 4200 TapeStation
886 (Agilent Technologies) and then libraries generated using the Illumina® Stranded mRNA Prep. Ligation
887 kit (Illumina, Inc.) according to the manufacturer's protocol. Briefly, total RNA (typically 0.025-1ug)
888 was used as input material from which polyadenylated mRNA was purified using poly-T, oligo-
889 attached, magnetic beads. Next, the mRNA was fragmented under elevated temperature and then
890 reverse transcribed into first strand cDNA using random hexamer primers and in the presence of
891 Actinomycin D (thus improving strand specificity whilst mitigating spurious DNA-dependent
892 synthesis). Following removal of the template RNA, second strand cDNA was then synthesized to yield
893 blunt-ended, double-stranded cDNA fragments. Strand specificity was maintained by the
894 incorporation of deoxyuridine triphosphate (dUTP) in place of dTTP to quench the second strand
895 during subsequent amplification. Following a single adenine (A) base addition, adapters with a
896 corresponding, complementary thymine (T) overhang were ligated to the cDNA fragments. Pre-index
897 anchors were then ligated to the ends of the double-stranded cDNA fragments to prepare them for
898 dual indexing. A subsequent PCR amplification step was then used to add the index adapter sequences
899 to create the final cDNA library. The adapter indices enabled the multiplexing of the libraries, which
900 were pooled prior to cluster generation using a cBot instrument. The loaded flow-cell was then paired-
901 end sequenced (76 + 76 cycles, plus indices) on an Illumina HiSeq4000 instrument. Finally, the output
902 data was demultiplexed and BCL-to-Fastq conversion performed using Illumina's bcl2fastq software,
903 version 2.20.0.422

904 **RNA-seq analysis**

905 Unmapped paired-reads of 76bp from the Illumina HiSeq4000 sequencer were checked using a quality
906 control pipeline consisting of FastQC v0.11.3
907 (http://www.bioinformatics.babraham.ac.uk/projects/fastqc/) and FastQ Screen v0.13.0
908 (https://www.bioinformatics.babraham.ac.uk/projects/fastq_screen/).

909 The reads were trimmed to remove any adapter or poor quality sequence using Trimmomatic v0.39
910 [121]; reads were truncated at a sliding 4bp window, starting 5', with a mean quality <Q20, and
911 removed if the final length was less than 35bp. Additional flags included: 'ILLUMINACLIP:./Truseq3-
912 PE-2_Nextera-PE.fa:2:30:10 SLIDINGWINDOW:4:20 MINLEN:35'.

913 The filtered reads were mapped either to the *Aspergillus fumigatus* A1163 reference sequence
914 (GCA_000150145.1/ASM15014v1) downloaded from the Ensembl Genomes Fungi v44 [122] or PD-
915 104 a *de novo* assembled genome, using STAR v5.3a [123]. For A1163 reference the genome index
916 was created using the GTF gene annotation also from Ensembl Genomes Fungi v44. For the PD-104
917 reference GTF gene annotation was generated as described below. A suitable flag for the read length
918 (--sjdbOverhang 75) was used. '--quantMode GeneCounts' was used to generate read counts in
919 genes.

920 Subsequently, PD-104 reads were aligned to the recently generated pan-genome [65] using Salmon
921 v1.6.0 (additional parameters for salmon quant: --gcBias (corrects for any GC biases in samples) -l ISR
922 (inward / stranded / reverse read pairs)).

923 Normalisation and differential expression analysis was performed using DESeq2 v1.34.0 [124] on R
924 v4.1.2 (R Core Team. 2021. R: A Language and Environment for Statistical Computing. https://www.R-
925 project.org/). Log fold change shrinkage was applied using the lfcShrink function along with the
926 "apeglm" algorithm [125].

927 The RNA data is stored in Array Express, accession E-MTAB-11547
928 (https://www.ebi.ac.uk/arrayexpress/experiments/E-MTAB-11547).

929

930 **DNA sequencing (Illumina DNA Prep)**

931 Genomic DNA was submitted to the Genomic Technologies Core Facility (GTCF) at the University of
932 Manchester. Sequencing libraries were generated using on-bead tagmentation chemistry with the
933 llumina® DNA Prep, (M) Tagmentation Kit (Illumina, Inc.) according to the manufacturer's protocol.
934 Briefly, bead-linked transposomes were used to mediate the simultaneous fragmentation of gDNA
935 (100-500ng) and the addition of Illumina sequencing primers. Next, reduced-cycle PCR amplification
936 was used to amplify sequencing ready DNA fragments and to add the indices and adapters. Finally,
937 sequencing-ready fragments were washed and pooled prior to paired-end sequencing (151 + 151

938 cycles, plus indices) on an Illumina NextSeq500 instrument. Finally, the output data were
939 demultiplexed (allowing one mismatch) and BCL-to-Fastq conversion performed using Illumina's
940 bcl2fastq software, version 2.20.0.422.

941 **Method for de novo genome assembly of genomes (PD-104 as example):**

942 Unmapped paired-end reads of 149bp from an Illumina NextSeq500 sequencer were checked using a
943 quality control pipeline consisting of FastQC v0.11.3
944 (http://www.bioinformatics.babraham.ac.uk/projects/fastqc/) and FastQ Screen v0.13.0
945 (https://www.bioinformatics.babraham.ac.uk/projects/fastq_screen/).
946 The reads were trimmed to remove any adapter or poor quality sequence using Trimmomatic v0.39
947 [121]. Within the first or last 30bp of a read bases were removed if quality was <30. A sliding 2bp
948 window, starting 5', scanned the reads and truncated at a window with a mean quality <Q20. Reads
949 were removed if the final length was less than 100bp. Additional flags included:
950 'ILLUMINACLIP:./Truseq3_Nextera-PE.fa:2:30:10 LEADING:30 TRAILING:30 SLIDINGWINDOW:2:20
951 MINLEN:100'.
952 Genome assembly was performed using Megahit v1.2.9 [126], using the flag '--no-mercy'. This
953 resulted in 799 contigs, total 28659847 bp, min 202 bp, max 401152 bp, avg 35869 bp, N50 97740
954 bp. In comparison A1163 has 55 contigs total 29205420 bp.
955 Quast v5.0.2 [127] was used to determine the quality of the assembly. An example of the PD-104
956 results can be found in Table S10 in https://doi.org/10.5281/zenodo.7021623.
957 ProtHint v2.5.0 and GeneMark-EP+ v4.68_lic [128] were used for gene annotation. ProtHint was used
958 to generate the evidence for coding genes in combination with fungal protein download from OrthoDb
959 v10. ProtHint generates two main outputs: `prothint.gff` a GFF file with all reported hints (introns,
960 starts and stops), and `evidence.gff` high confidence subset of `prothint.gff` which is suitable for the
961 GeneMark-EP Plus mode. GeneMark-EP+ was used to generate a GTF file of candidate genes for the
962 PD-104 assembly. Additional parameters were set '--max_intron 200 --max_intergenic 100000 --
963 min_contig=1000 --fungus'.
964 In order to determine the function of the novel genes, initially a reciprocal best hit strategy was used
965 comparing protein sequence from PD-104 (using the GeneMark Perl script
966 'get_sequence_from_GTF.pl' with the GTF file and assembled contigs) and A1163 (proteins
967 downloaded from Ensembl Genomes Fungi release 51:
968 http://ftp.ensemblgenomes.org/pub/fungi/release-
969 51/fasta/aspergillus_fumigatusa1163/pep/Aspergillus_fumigatusa1163.ASM15014v1.pep.all.fa.gz).
970 The best match method was run using proteinortho v6.0.31 [129], which by default uses the program

971 Diamond v2.0.13 [130] to identify protein matches ('-p=diamond'). The flag '-sim=1' was set to obtain
972 best reciprocal matches only.

973 **Construction of Phylogenetic tree:**

974 Pre-alignment, the reference Af293 genome [131] was masked to remove low-complexity regions
975 using RepeatMasker (http://www.repeatmasker.org/) v.4.1.2-p1 and the Dfam repeat database [132]
976 release 3.5. Quality-checked DNA sequencing reads from the recently generated pan-genome study
977 [65] were combined with the reads generated from this study and underwent alignment to the
978 masked reference Af293 genome, using BWA-MEM [133] v.0.7.17-r1188. Alignment files were then
979 converted to the sorted BAM format using SAMtools [134] v.1.10. Variant calling was then performed
980 with GATK HaplotypeCaller [135] v.4.0. All variant calls with a genotype quality less than 50 were
981 removed and low-confidence SNPs were converted to missing data if they met one of the follow
982 criteria: DP < 10 || RMSMappingQuality < 40.0 || QualByDepth < 2.0 || FisherStrand > 60.0 ||
983 ABHom < 0.9. Each newly generated VCF file was then compressed, indexed and then merged into a
984 single file using VCFtools [136] v.0.1.16. This data was then converted into a relaxed interleaved Phylip
985 format using vcf2phylip [137] v2.8 and RAxML [138] v.8.2.12, under rapid bootstrap analysis using
986 1,000 replicates with the GTRCAT model, was employed to generate maximum-likelihood phylogenies
987 to test whether persistence is lineage-specific. Phylogenetic trees with overlaying metadata were
988 generated using iTOL [139] v.6.5.4.

989 **ACKNOWLEGDGEMENTS**

990 We are deeply grateful to Prof Paul Dyer, who kindly gifted to us the collection of isolates that have
991 been used in this study. We would like to thank Diego Megías and Clara Martín at ISCIII for their help
992 with the microscopy. We are also grateful to Michael Bottery for relevant conversations about
993 bacterial tolerance and persistence. We acknowledge the use of the Genomic Technologies Facility
994 (Faculty of Biology Medicine and Health, University of Manchester) for the DNA and RNA sequencing.
995 Help and support from members of MFIG and LRIM is greatly appreciated.

996 JA is funded by an Atracción de Talento Modalidad 1 (020-T1/BMD-200) contract of the Madrid
997 Regional Government (CAM). JS has been funded by a BSAC Scholarship (bsac-2016-0049). CV was
998 funded by FAPESP (2108/00715-3 and 2020/01131-5). GHG has been funded by FAPESP (2016/07870-
999 9 and 2021/04977-5), CNPq (301058/2019-9 and 404735/2018-5) and by the NIH/NIAID (grant no.
1000 R01AI153356). SG was co-funded by the NIHR Manchester Research Centre and the Fungal Infection
1001 Trust.

1002

1003 **DATA AVAILABILITY**

Transcriptomic data is available in Array Express (https://www.ebi.ac.uk/arrayexpress/experiments/E-MTAB-11547). All raw data is available upon reasonable request.

## REFERENCES


1. Latgé, J.-P. and G. Chamilos, *Aspergillus fumigatus and Aspergillosis in 2019.* Clinical Microbiology Reviews, 2019. **33**(1) DOI: 10.1128/cmr.00140-18.
2. Perfect, J.R., *The antifungal pipeline: a reality check.* Nat Rev Drug Discov, 2017. **16**(9): p. 603-616 DOI: 10.1038/nrd.2017.46.
3. Ruping, M.J., J.J. Vehreschild, and O.A. Cornely, *Antifungal treatment strategies in high risk patients.* Mycoses, 2008. **51 Suppl 2**: p. 46-51 DOI: 10.1111/j.1439-0507.2008.01572.x.
4. Koehler, P., et al., *Defining and managing COVID-19-associated pulmonary aspergillosis: the 2020 ECMM/ISHAM consensus criteria for research and clinical guidance.* The Lancet Infectious Diseases, 2021. **21**(6): p. e149-e162 DOI: 10.1016/s1473-3099(20)30847-1.
5. Marr, K.A., et al., *Aspergillosis Complicating Severe Coronavirus Disease.* Emerging Infectious Diseases, 2021. **27**(1): p. 18-25 DOI: 10.3201/eid2701.202896.
6. Helleberg, M., M. Steensen, and M.C. Arendrup, *Invasive aspergillosis in patients with severe COVID-19 pneumonia.* Clinical Microbiology and Infection, 2021. **27**(1): p. 147-148 DOI: 10.1016/j.cmi.2020.07.047.
7. Lowes, D., et al., *Predictors of mortality in chronic pulmonary aspergillosis.* Eur Respir J, 2017. **49**(2) DOI: 10.1183/13993003.01062-2016.
8. Brown, G.D., et al., *Hidden killers: human fungal infections.* Sci Transl Med, 2012. **4**(165): p. 165rv13 DOI: 10.1126/scitranslmed.3004404.
9. Ballou, L., *Fungal diseases deserve our attention.* Nature Microbiology Community, 2017. **http://go.nature.com/2jlKFYZ**.
10. Fisher, M.C., et al., *Worldwide emergence of resistance to antifungal drugs challenges human health and food security.* Science, 2018. **360**(6390): p. 739-742 DOI: 10.1126/science.aap7999.
11. Verweij, P.E., et al., *International expert opinion on the management of infection caused by azole-resistant Aspergillus fumigatus.* Drug Resist Updat, 2015. **21-22**: p. 30-40 DOI: 10.1016/j.drup.2015.08.001.
12. Lestrade, P.P., et al., *Voriconazole Resistance and Mortality in Invasive Aspergillosis: A Multicenter Retrospective Cohort Study.* Clin Infect Dis, 2019. **68**(9): p. 1463-1471 DOI: 10.1093/cid/ciy859.
13. Meis, J.F., et al., *Clinical implications of globally emerging azole resistance in Aspergillus fumigatus.* Philos Trans R Soc Lond B Biol Sci, 2016. **371**(1709) DOI: 10.1098/rstb.2015.0460.
14. Galiger, C., et al., *Assessment of efficacy of antifungals against Aspergillus fumigatus: value of real-time bioluminescence imaging.* Antimicrob Agents Chemother, 2013. **57**(7): p. 3046-59 DOI: 10.1128/AAC.01660-12.
15. Heo, S.T., et al., *Changes in In Vitro Susceptibility Patterns of Aspergillus to Triazoles and Correlation With Aspergillosis Outcome in a Tertiary Care Cancer Center, 1999–2015.* Clinical Infectious Diseases, 2017. **65**(2): p. 216-225 DOI: 10.1093/cid/cix297.
16. Leong, J.M., et al., *Antibiotic tolerance.* PLOS Pathogens, 2020. **16**(10) DOI: 10.1371/journal.ppat.1008892.
17. Levinson, T., et al., *Impact of tolerance to fluconazole on treatment response in Candida albicans bloodstream infection.* Mycoses, 2020. **64**(1): p. 78-85 DOI: 10.1111/myc.13191.
18. Brauner, A., et al., *Distinguishing between resistance, tolerance and persistence to antibiotic treatment.* Nature Reviews Microbiology, 2016. **14**(5): p. 320-330 DOI: 10.1038/nrmicro.2016.34.

1052 19. Balaban, N.Q., et al., *Definitions and guidelines for research on antibiotic persistence.* Nature
1053 Reviews Microbiology, 2019. **17**(7): p. 441-448 DOI: 10.1038/s41579-019-0196-3.
1054 20. Meylan, S., I.W. Andrews, and J.J. Collins, *Targeting Antibiotic Tolerance, Pathogen by*
1055 *Pathogen.* Cell, 2018. **172**(6): p. 1228-1238 DOI: 10.1016/j.cell.2018.01.037.
1056 21. Rosenberg, A., et al., *Antifungal tolerance is a subpopulation effect distinct from resistance*
1057 *and is associated with persistent candidemia.* Nature Communications, 2018. **9**(1) DOI:
1058 10.1038/s41467-018-04926-x.
1059 22. Martos, A.I., et al., *Evaluation of the Etest method for susceptibility testing of Aspergillus spp.*
1060 *and Fusarium spp. to three echinocandins.* Med Mycol, 2010. **48**(6): p. 858-61 DOI:
1061 10.3109/13693781003586943.
1062 23. Lass-Florl, C., et al., *Antifungal susceptibility testing in Aspergillus spp. according to EUCAST*
1063 *methodology.* Med Mycol, 2006. **44**(Supplement_1): p. S319-S325 DOI:
1064 10.1080/13693780600779401.
1065 24. Bleichrodt, R.J., et al., *Cell Wall Composition Heterogeneity between Single Cells in Aspergillus*
1066 *fumigatus Leads to Heterogeneous Behavior during Antifungal Treatment and Phagocytosis.*
1067 mBio, 2020. **11**(3) DOI: 10.1128/mBio.03015-19.
1068 25. Wagener, J. and V. Loiko, *Recent Insights into the Paradoxical Effect of Echinocandins.* Journal
1069 of Fungi, 2017. **4**(1) DOI: 10.3390/jof4010005.
1070 26. Valero, C., et al., *The Caspofungin Paradoxical Effect is a Tolerant "Eagle Effect" in the*
1071 *Filamentous Fungal Pathogen Aspergillus fumigatus.* mBio, 2022 DOI: 10.1128/mbio.00447-
1072 22.
1073 27. Aruanno, M., E. Glampedakis, and F. Lamoth, *Echinocandins for the Treatment of Invasive*
1074 *Aspergillosis: from Laboratory to Bedside.* Antimicrobial Agents and Chemotherapy, 2019.
1075 **63**(8) DOI: 10.1128/aac.00399-19.
1076 28. Gheith, S., et al., *In vitro susceptibility to amphotericin B, itraconazole, voriconazole,*
1077 *posaconazole and caspofungin of Aspergillus spp. isolated from patients with haematological*
1078 *malignancies in Tunisia.* Springerplus, 2014. **3**: p. 19 DOI: 10.1186/2193-1801-3-19.
1079 29. Geißel, B., et al., *Azole-induced cell wall carbohydrate patches kill Aspergillus fumigatus.*
1080 Nature Communications, 2018. **9**(1) DOI: 10.1038/s41467-018-05497-7.
1081 30. Majoros, L. and G. Kardos, *Fungicidal Activity of Azole Antifungal Agents.* Anti-Infective Agents
1082 in Medicinal Chemistry, 2008. **7**(2): p. 118-125 DOI: 10.2174/187152108783954623.
1083 31. Manavathu, E.K., J.L. Cutright, and P.H. Chandrasekar, *Organism-Dependent Fungicidal*
1084 *Activities of Azoles.* Antimicrobial Agents and Chemotherapy, 1998. **42**(11): p. 3018-3021 DOI:
1085 10.1128/aac.42.11.3018.
1086 32. Wang, F., et al., *Transcription in fungal conidia before dormancy produces phenotypically*
1087 *variable conidia that maximize survival in different environments.* Nature Microbiology, 2021.
1088 **6**(8): p. 1066-1081 DOI: 10.1038/s41564-021-00922-y.
1089 33. Dannaoui, E. and A. Espinel-Ingroff, *Antifungal Susceptibly Testing by Concentration Gradient*
1090 *Strip Etest Method for Fungal Isolates: A Review.* Journal of Fungi, 2019. **5**(4) DOI:
1091 10.3390/jof5040108.
1092 34. Gefen, O., et al., *TDtest: easy detection of bacterial tolerance and persistence in clinical isolates*
1093 *by a modified disk-diffusion assay.* Sci Rep, 2017. **7**: p. 41284 DOI: 10.1038/srep41284.
1094 35. Gonzalez-Jimenez, I., et al., *Are Point Mutations in HMG-CoA Reductases (Hmg1 and Hmg2) a*
1095 *Step towards Azole Resistance in Aspergillus fumigatus?* Molecules, 2021. **26**(19) DOI:
1096 10.3390/molecules26195975.
1097 36. Zhang, J., et al., *Evolution of cross-resistance to medical triazoles in Aspergillus fumigatus*
1098 *through selection pressure of environmental fungicides.* Proceedings of the Royal Society B:
1099 Biological Sciences, 2017. **284**(1863) DOI: 10.1098/rspb.2017.0635.
1100 37. Windels, E.M., et al., *Bacterial persistence promotes the evolution of antibiotic resistance by*
1101 *increasing survival and mutation rates.* The ISME Journal, 2019. **13**(5): p. 1239-1251 DOI:
1102 10.1038/s41396-019-0344-9.

1103 38. Sebastian, J., et al., *De Novo Emergence of Genetically Resistant Mutants of Mycobacterium*
1104 *tuberculosis from the Persistence Phase Cells Formed against Antituberculosis Drugs In Vitro.*
1105 Antimicrobial Agents and Chemotherapy, 2017. **61**(2) DOI: 10.1128/aac.01343-16.
1106 39. Suh, M.-J., et al., *Development stage-specific proteomic profiling uncovers small, lineage*
1107 *specific proteins most abundant in the Aspergillus fumigatus conidial proteome.* Proteome
1108 Science, 2012. **10**(1) DOI: 10.1186/1477-5956-10-30.
1109 40. Kubitschek-Barreira, P.H., et al., *Differential proteomic analysis of Aspergillus fumigatus*
1110 *morphotypes reveals putative drug targets.* Journal of Proteomics, 2013. **78**: p. 522-534 DOI:
1111 10.1016/j.jprot.2012.10.022.
1112 41. McDonagh, A., et al., *Sub-Telomere Directed Gene Expression during Initiation of Invasive*
1113 *Aspergillosis.* PLoS Pathogens, 2008. **4**(9) DOI: 10.1371/journal.ppat.1000154.
1114 42. Mowat, E., et al., *Phase-dependent antifungal activity against Aspergillus fumigatus*
1115 *developing multicellular filamentous biofilms.* Journal of Antimicrobial Chemotherapy, 2008.
1116 **62**(6): p. 1281-1284 DOI: 10.1093/jac/dkn402.
1117 43. Yu, J.S.L., et al., *Microbial communities form rich extracellular metabolomes that foster*
1118 *metabolic interactions and promote drug tolerance.* Nature Microbiology, 2022. **7**(4): p. 542-
1119 555 DOI: 10.1038/s41564-022-01072-5.
1120 44. Day, A.M. and J. Quinn, *Stress-Activated Protein Kinases in Human Fungal Pathogens.* Frontiers
1121 in Cellular and Infection Microbiology, 2019. **9** DOI: 10.3389/fcimb.2019.00261.
1122 45. Hagiwara, D., et al., *Signaling pathways for stress responses and adaptation in Aspergillus*
1123 *species: stress biology in the post-genomic era.* Bioscience, Biotechnology, and Biochemistry,
1124 2016. **80**(9): p. 1667-1680 DOI: 10.1080/09168451.2016.1162085.
1125 46. Manfiolli, A.O., et al., *Aspergillus fumigatus High Osmolarity Glycerol Mitogen Activated*
1126 *Protein Kinases SakA and MpkC Physically Interact During Osmotic and Cell Wall Stresses.*
1127 Frontiers in Microbiology, 2019. **10** DOI: 10.3389/fmicb.2019.00918.
1128 47. Takahashi, H., et al., *Global gene expression reveals stress-responsive genes in Aspergillus*
1129 *fumigatus mycelia.* BMC Genomics, 2017. **18**(1) DOI: 10.1186/s12864-017-4316-z.
1130 48. Berman, J. and D.J. Krysan, *Drug resistance and tolerance in fungi.* Nat Rev Microbiol, 2020
1131 DOI: 10.1038/s41579-019-0322-2.
1132 49. Cowen, L.E., et al., *Harnessing Hsp90 function as a powerful, broadly effective therapeutic*
1133 *strategy for fungal infectious disease.* Proceedings of the National Academy of Sciences, 2009.
1134 **106**(8): p. 2818-2823 DOI: 10.1073/pnas.0813394106.
1135 50. Lamoth, F., et al., *Antifungal activity of compounds targeting the Hsp90-calcineurin pathway*
1136 *against various mould species.* Journal of Antimicrobial Chemotherapy, 2015. **70**(5): p. 1408-
1137 1411 DOI: 10.1093/jac/dku549.
1138 51. Juvvadi, P.R., F. Lamoth, and W.J. Steinbach, *Calcineurin as a multifunctional regulator:*
1139 *Unraveling novel functions in fungal stress responses, hyphal growth, drug resistance, and*
1140 *pathogenesis.* Fungal Biology Reviews, 2014. **28**(2-3): p. 56-69 DOI: 10.1016/j.fbr.2014.02.004.
1141 52. Sestari, S.J., et al., *Inhibition of protein kinase A affects Paracoccidioides lutzii dimorphism.*
1142 International Journal of Biological Macromolecules, 2018. **113**: p. 1214-1220 DOI:
1143 10.1016/j.ijbiomac.2018.03.023.
1144 53. Chen, S.C.A., R.E. Lewis, and D.P. Kontoyiannis, *Direct effects of non-antifungal agents used in*
1145 *cancer chemotherapy and organ transplantation on the development and virulence of Candida*
1146 *and Aspergillus species.* Virulence, 2014. **2**(4): p. 280-295 DOI: 10.4161/viru.2.4.16764.
1147 54. Weichert, M., et al., *Functional Coupling between the Unfolded Protein Response and*
1148 *Endoplasmic Reticulum/Golgi Ca2+-ATPases Promotes Stress Tolerance, Cell Wall Biosynthesis,*
1149 *and Virulence of Aspergillus fumigatus.* mBio, 2020. **11**(3) DOI: 10.1128/mBio.01060-20.
1150 55. Istvan, E.S., *Structural Mechanism for Statin Inhibition of HMG-CoA Reductase.* Science, 2001.
1151 **292**(5519): p. 1160-1164 DOI: 10.1126/science.1059344.
1152 56. Qiao, J., et al., *Antifungal activity of statins against Aspergillus species.* Med Mycol, 2007.
1153 **45**(7): p. 589-93 DOI: 10.1080/13693780701397673.

1154 57. Silva, L.V., et al., *Milbemycins: More than Efflux Inhibitors for Fungal Pathogens.* Antimicrobial
1155 Agents and Chemotherapy, 2012. **57**(2): p. 873-886 DOI: 10.1128/aac.02040-12.
1156 58. Esquivel, B.D., et al., *Characterization of the Efflux Capability and Substrate Specificity of*
1157 *Aspergillus fumigatus PDR5-like ABC Transporters Expressed in Saccharomyces cerevisiae.*
1158 mBio, 2020. **11**(2) DOI: 10.1128/mBio.00338-20.
1159 59. Gonzalez-Jimenez, I., et al., *A Cyp51B Mutation Contributes to Azole Resistance in Aspergillus*
1160 *fumigatus.* Journal of Fungi, 2020. **6**(4) DOI: 10.3390/jof6040315.
1161 60. Rybak, J.M., et al., *Mutations in hmg1, Challenging the Paradigm of Clinical Triazole Resistance*
1162 *in Aspergillus fumigatus.* mBio, 2019. **10**(2) DOI: 10.1128/mBio.00437-19.
1163 61. Furukawa, T., et al., *The negative cofactor 2 complex is a key regulator of drug resistance in*
1164 *Aspergillus fumigatus.* Nat Commun, 2020. **11**(1): p. 427 DOI: 10.1038/s41467-019-14191-1.
1165 62. Hulsen, T., J. de Vlieg, and W. Alkema, *BioVenn - a web application for the comparison and*
1166 *visualization of biological lists using area-proportional Venn diagrams.* BMC Genomics, 2008.
1167 **9**: p. 488 DOI: 10.1186/1471-2164-9-488.
1168 63. Amos, B., et al., *VEuPathDB: the eukaryotic pathogen, vector and host bioinformatics resource*
1169 *center.* Nucleic Acids Research, 2022. **50**(D1): p. D898-D911 DOI: 10.1093/nar/gkab929.
1170 64. Peyrusson, F., et al., *Intracellular Staphylococcus aureus persisters upon antibiotic exposure.*
1171 Nature Communications, 2020. **11**(1) DOI: 10.1038/s41467-020-15966-7.
1172 65. Rhodes, J., et al., *Population genomics confirms acquisition of drug-resistant Aspergillus*
1173 *fumigatus infection by humans from the environment.* Nature Microbiology, 2022 DOI:
1174 10.1038/s41564-022-01091-2.
1175 66. Szklarczyk, D., et al., *The STRING database in 2021: customizable protein-protein networks,*
1176 *and functional characterization of user-uploaded gene/measurement sets.* Nucleic Acids Res,
1177 2021. **49**(D1): p. D605-D612 DOI: 10.1093/nar/gkaa1074.
1178 67. Supek, F., et al., *REVIGO Summarizes and Visualizes Long Lists of Gene Ontology Terms.* PLoS
1179 ONE, 2011. **6**(7) DOI: 10.1371/journal.pone.0021800.
1180 68. Rossi, N.A., I. El Meouche, and M.J. Dunlop, *Forecasting cell fate during antibiotic exposure*
1181 *using stochastic gene expression.* Communications Biology, 2019. **2**(1) DOI: 10.1038/s42003-
1182 019-0509-0.
1183 69. Urbaniec, J., et al., *Phenotypic heterogeneity in persisters: a novel 'hunker' theory of*
1184 *persistence.* FEMS Microbiology Reviews, 2022. **46**(1) DOI: 10.1093/femsre/fuab042.
1185 70. Fraczek, M.G., et al., *The cdr1B efflux transporter is associated with non-cyp51a-mediated*
1186 *itraconazole resistance in Aspergillus fumigatus* Journal of Antimicrobial Chemotherapy, 2013.
1187 **68**(7): p. 1486-1496 DOI: 10.1093/jac/dkt075.
1188 71. Bamford, N.C., et al., *Sph3 Is a Glycoside Hydrolase Required for the Biosynthesis of*
1189 *Galactosaminogalactan in Aspergillus fumigatus.* Journal of Biological Chemistry, 2015.
1190 **290**(46): p. 27438-27450 DOI: 10.1074/jbc.M115.679050.
1191 72. Lee, M.J., et al., *Deacetylation of Fungal Exopolysaccharide Mediates Adhesion and Biofilm*
1192 *Formation.* mBio, 2016. **7**(2) DOI: 10.1128/mBio.00252-16.
1193 73. Bromley, M.J., et al., *Occurrence of azole-resistant species of Aspergillus in the UK*
1194 *environment.* J Glob Antimicrob Resist, 2014. **2**(4): p. 276-279 DOI:
1195 10.1016/j.jgar.2014.05.004.
1196 74. Gonzalez-Jimenez, I., et al., *Multiresistance to Nonazole Fungicides in Aspergillus fumigatus*
1197 *TR34/L98H Azole-Resistant Isolates.* Antimicrobial Agents and Chemotherapy, 2021. **65**(9)
1198 DOI: 10.1128/aac.00642-21.
1199 75. Forastiero, A., et al., *In vivo efficacy of voriconazole and posaconazole therapy in a novel*
1200 *invertebrate model of Aspergillus fumigatus infection.* International Journal of Antimicrobial
1201 Agents, 2015. **46**(5): p. 511-517 DOI: 10.1016/j.ijantimicag.2015.07.007.
1202 76. Gomez-Lopez, A., et al., *An invertebrate model to evaluate virulence in Aspergillus fumigatus:*
1203 *The role of azole resistance.* Medical Mycology, 2014. **52**(3): p. 311-319 DOI:
1204 10.1093/mmy/myt022.

1205 77. Jemel, S., et al., *In Vivo Efficacy of Voriconazole in a Galleria mellonella Model of Invasive*
1206 *Infection Due to Azole-Susceptible or Resistant Aspergillus fumigatus Isolates.* Journal of Fungi,
1207 2021. **7**(12) DOI: 10.3390/jof7121012.
1208 78. Hobby, G.L., K. Meyer, and E. Chaffee, *Observations on the Mechanism of Action of Penicillin.*
1209 Experimental Biology and Medicine, 1942. **50**(2): p. 281-285 DOI: 10.3181/00379727-50-
1210 13773.
1211 79. Bigger, J., *Treatment of Staphylococcal Infections with Penicillin by Intermittent Sterilisation.*
1212 The Lancet, 1944. **244**(6320): p. 497-500 DOI: 10.1016/s0140-6736(00)74210-3.
1213 80. Cohen, Nadia R., Michael A. Lobritz, and James J. Collins, *Microbial Persistence and the Road*
1214 *to Drug Resistance.* Cell Host & Microbe, 2013. **13**(6): p. 632-642 DOI:
1215 10.1016/j.chom.2013.05.009.
1216 81. Huemer, M., et al., *Antibiotic resistance and persistence—Implications for human health and*
1217 *treatment perspectives.* EMBO reports, 2020. **21**(12) DOI: 10.15252/embr.202051034.
1218 82. LaFleur, M.D., C.A. Kumamoto, and K. Lewis, *Candida albicans Biofilms Produce Antifungal-*
1219 *Tolerant Persister Cells.* Antimicrobial Agents and Chemotherapy, 2006. **50**(11): p. 3839-3846
1220 DOI: 10.1128/aac.00684-06.
1221 83. Hobman, T.C., et al., *Fungal persister cells: The basis for recalcitrant infections?* PLOS
1222 Pathogens, 2018. **14**(10) DOI: 10.1371/journal.ppat.1007301.
1223 84. Kowalski, C.H., et al., *Fungal biofilm architecture produces hypoxic microenvironments that*
1224 *drive antifungal resistance.* Proceedings of the National Academy of Sciences, 2020. **117**(36):
1225 p. 22473-22483 DOI: 10.1073/pnas.2003700117.
1226 85. Wilmaerts, D., et al., *General Mechanisms Leading to Persister Formation and Awakening.*
1227 Trends in Genetics, 2019. **35**(6): p. 401-411 DOI: 10.1016/j.tig.2019.03.007.
1228 86. Orman, M.A. and M.P. Brynildsen, *Dormancy Is Not Necessary or Sufficient for Bacterial*
1229 *Persistence.* Antimicrobial Agents and Chemotherapy, 2013. **57**(7): p. 3230-3239 DOI:
1230 10.1128/aac.00243-13.
1231 87. Wakamoto, Y., et al., *Dynamic Persistence of Antibiotic-Stressed Mycobacteria.* Science, 2013.
1232 **339**(6115): p. 91-95 DOI: 10.1126/science.1229858.
1233 88. Claudi, B., et al., *Phenotypic Variation of Salmonella in Host Tissues Delays Eradication by*
1234 *Antimicrobial Chemotherapy.* Cell, 2014. **158**(4): p. 722-733 DOI: 10.1016/j.cell.2014.06.045.
1235 89. Stapels, D.A.C., et al., *Salmonella persisters undermine host immune defenses during antibiotic*
1236 *treatment.* Science, 2018. **362**(6419): p. 1156-1160 DOI: 10.1126/science.aat7148.
1237 90. Li, P., et al., *Delicate Metabolic Control and Coordinated Stress Response Critically Determine*
1238 *Antifungal Tolerance of Candida albicans Biofilm Persisters.* Antimicrobial Agents and
1239 Chemotherapy, 2015. **59**(10): p. 6101-6112 DOI: 10.1128/aac.00543-15.
1240 91. Monteiro, M.C., et al., *A New Approach to Drug Discovery: High-Throughput Screening of*
1241 *Microbial Natural Extracts against Aspergillus fumigatus Using Resazurin* Journal of
1242 Biomolecular Screening, 2012. **17**(4): p. 542-549 DOI: 10.1177/1087057111433459.
1243 92. Hillmann, F., E. Shekhova, and O. Kniemeyer, *Insights into the cellular responses to hypoxia in*
1244 *filamentous fungi.* Current Genetics, 2015. **61**(3): p. 441-455 DOI: 10.1007/s00294-015-0487-
1245 9.
1246 93. Trastoy, R., et al., *Mechanisms of Bacterial Tolerance and Persistence in the Gastrointestinal*
1247 *and Respiratory Environments.* Clinical Microbiology Reviews, 2018. **31**(4) DOI:
1248 10.1128/cmr.00023-18.
1249 94. Barber, A.E., et al., *Aspergillus fumigatus pan-genome analysis identifies genetic variants*
1250 *associated with human infection.* Nature Microbiology, 2021. **6**(12): p. 1526-1536 DOI:
1251 10.1038/s41564-021-00993-x.
1252 95. Manuse, S., et al., *Bacterial persisters are a stochastically formed subpopulation of low-energy*
1253 *cells.* PLOS Biology, 2021. **19**(4) DOI: 10.1371/journal.pbio.3001194.
1254 96. Zalis, E.A., et al., *Stochastic Variation in Expression of the Tricarboxylic Acid Cycle Produces*
1255 *Persister Cells.* mBio, 2019. **10**(5) DOI: 10.1128/mBio.01930-19.

1256 97. El Meouche, I., Y. Siu, and M.J. Dunlop, *Stochastic expression of a multiple antibiotic resistance*
1257 *activator confers transient resistance in single cells.* Scientific Reports, 2016. **6**(1) DOI:
1258 10.1038/srep19538.
1259 98. Pu, Y., et al., *Enhanced Efflux Activity Facilitates Drug Tolerance in Dormant Bacterial Cells.*
1260 Molecular Cell, 2016. **62**(2): p. 284-294 DOI: 10.1016/j.molcel.2016.03.035.
1261 99. Fontaine, T., et al., *Galactosaminogalactan, a New Immunosuppressive Polysaccharide of*
1262 *Aspergillus fumigatus.* PLoS Pathogens, 2011. **7**(11) DOI: 10.1371/journal.ppat.1002372.
1263 100. Speth, C., et al., *Galactosaminogalactan (GAG) and its multiple roles in Aspergillus*
1264 *pathogenesis.* Virulence, 2019. **10**(1): p. 976-983 DOI: 10.1080/21505594.2019.1568174.
1265 101. Fisher, R.A., B. Gollan, and S. Helaine, *Persistent bacterial infections and persister cells.* Nature
1266 Reviews Microbiology, 2017. **15**(8): p. 453-464 DOI: 10.1038/nrmicro.2017.42.
1267 102. Mondon, P., et al., *Heteroresistance to fluconazole and voriconazole in Cryptococcus*
1268 *neoformans.* Antimicrob Agents Chemother, 1999. **43**(8): p. 1856-61 DOI:
1269 10.1128/AAC.43.8.1856.
1270 103. Yamazumi, T., et al., *Characterization of Heteroresistance to Fluconazole among Clinical*
1271 *Isolates of Cryptococcus neoformans.* Journal of Clinical Microbiology, 2003. **41**(1): p. 267-272
1272 DOI: 10.1128/jcm.41.1.267-272.2003.
1273 104. Varma, A. and K.J. Kwon-Chung, *Heteroresistance of Cryptococcus gattii to Fluconazole.*
1274 Antimicrobial Agents and Chemotherapy, 2010. **54**(6): p. 2303-2311 DOI: 10.1128/aac.00153-
1275 10.
1276 105. Stone, N.R.H., et al., *Dynamic ploidy changes drive fluconazole resistance in human*
1277 *cryptococcal meningitis.* Journal of Clinical Investigation, 2019. **129**(3): p. 999-1014 DOI:
1278 10.1172/jci124516.
1279 106. Barsh, G.S., et al., *A non-canonical RNA degradation pathway suppresses RNAi-dependent*
1280 *epimutations in the human fungal pathogen Mucor circinelloides.* PLOS Genetics, 2017. **13**(3)
1281 DOI: 10.1371/journal.pgen.1006686.
1282 107. Ferreira, G.F. and D.A. Santos, *Heteroresistance and fungi.* Mycoses, 2017. **60**(9): p. 562-568
1283 DOI: 10.1111/myc.12639.
1284 108. Sionov, E., et al., *Heteroresistance to Fluconazole in Cryptococcus neoformans Is Intrinsic and*
1285 *Associated with Virulence.* Antimicrobial Agents and Chemotherapy, 2009. **53**(7): p. 2804-
1286 2815 DOI: 10.1128/aac.00295-09.
1287 109. Todd, R.T. and A. Selmecki, *Expandable and reversible copy number amplification drives rapid*
1288 *adaptation to antifungal drugs.* eLife, 2020. **9** DOI: 10.7554/eLife.58349.
1289 110. Windels, E.M., et al., *Antibiotics: Combatting Tolerance To Stop Resistance.* mBio, 2019. **10**(5)
1290 DOI: 10.1128/mBio.02095-19.
1291 111. Tashiro, M., et al., *Correlation between Triazole Treatment History and Susceptibility in*
1292 *Clinically Isolated Aspergillus fumigatus.* Antimicrobial Agents and Chemotherapy, 2012.
1293 **56**(9): p. 4870-4875 DOI: 10.1128/Aac.00514-12.
1294 112. Kamei, K., et al., *High detection rate of azole-resistant Aspergillus fumigatus after treatment*
1295 *with azole antifungal drugs among patients with chronic pulmonary aspergillosis in a single*
1296 *hospital setting with low azole resistance.* Medical Mycology, 2020 DOI:
1297 10.1093/mmy/myaa052.
1298 113. Bertuzzi, M., et al., *On the lineage of Aspergillus fumigatus isolates in common laboratory use.*
1299 Medical Mycology, 2021. **59**(1): p. 7-13 DOI: 10.1093/mmy/myaa075.
1300 114. Swilaiman, S.S., et al., *Global Sexual Fertility in the Opportunistic Pathogen Aspergillus*
1301 *fumigatus and Identification of New Supermater Strains.* J Fungi (Basel), 2020. **6**(4) DOI:
1302 10.3390/jof6040258.
1303 115. Moreno, M.A., et al., *Culture conditions for zinc- and pH-regulated gene expression studies in*
1304 *Aspergillus fumigatus.* Int Microbiol, 2007. **10**(3): p. 187-92.

116. Gressler, M., et al., *Definition of the Anti-inflammatory Oligosaccharides Derived From the Galactosaminogalactan (GAG) From Aspergillus fumigatus.* Frontiers in Cellular and Infection Microbiology, 2019. **9** DOI: 10.3389/fcimb.2019.00365.
117. Papastamoulis, P., et al., *Bayesian Detection of Piecewise Linear Trends in Replicated Time-Series with Application to Growth Data Modelling.* The International Journal of Biostatistics, 2020. **16**(1) DOI: 10.1515/ijb-2018-0052.
118. Arendrup, M.C., et al., *EUCAST technical note on isavuconazole breakpoints for Aspergillus, itraconazole breakpoints for Candida and updates for the antifungal susceptibility testing method documents.* Clinical Microbiology and Infection, 2016. **22**(6): p. 571.e1-571.e4 DOI: 10.1016/j.cmi.2016.01.017.
119. Schindelin, J., et al., *Fiji: an open-source platform for biological-image analysis.* Nature Methods, 2012. **9**(7): p. 676-682 DOI: 10.1038/nmeth.2019.
120. Scott, J., et al., *Pseudomonas aeruginosa-Derived Volatile Sulfur Compounds Promote Distal Aspergillus fumigatus Growth and a Synergistic Pathogen-Pathogen Interaction That Increases Pathogenicity in Co-infection.* Front Microbiol, 2019. **10**: p. 2311 DOI: 10.3389/fmicb.2019.02311.
121. Bolger, A.M., M. Lohse, and B. Usadel, *Trimmomatic: a flexible trimmer for Illumina sequence data.* Bioinformatics, 2014. **30**(15): p. 2114-2120 DOI: 10.1093/bioinformatics/btu170.
122. Howe, K.L., et al., *Ensembl Genomes 2020—enabling non-vertebrate genomic research.* Nucleic Acids Research, 2020. **48**(D1): p. D689-D695 DOI: 10.1093/nar/gkz890.
123. Dobin, A., et al., *STAR: ultrafast universal RNA-seq aligner.* Bioinformatics, 2013. **29**(1): p. 15-21 DOI: 10.1093/bioinformatics/bts635.
124. Love, M.I., W. Huber, and S. Anders, *Moderated estimation of fold change and dispersion for RNA-seq data with DESeq2.* Genome Biology, 2014. **15**(12) DOI: 10.1186/s13059-014-0550-8.
125. Zhu, A., et al., *Heavy-tailed prior distributions for sequence count data: removing the noise and preserving large differences.* Bioinformatics, 2019. **35**(12): p. 2084-2092 DOI: 10.1093/bioinformatics/bty895.
126. Li, D., et al., *MEGAHIT: an ultra-fast single-node solution for large and complex metagenomics assembly via succinct de Bruijn graph.* Bioinformatics, 2015. **31**(10): p. 1674-1676 DOI: 10.1093/bioinformatics/btv033.
127. Gurevich, A., et al., *QUAST: quality assessment tool for genome assemblies.* Bioinformatics, 2013. **29**(8): p. 1072-1075 DOI: 10.1093/bioinformatics/btt086.
128. Brůna, T., A. Lomsadze, and M. Borodovsky, *GeneMark-EP+: eukaryotic gene prediction with self-training in the space of genes and proteins.* NAR Genomics and Bioinformatics, 2020. **2**(2) DOI: 10.1093/nargab/lqaa026.
129. Lechner, M., et al., *Proteinortho: Detection of (Co-)orthologs in large-scale analysis.* BMC Bioinformatics, 2011. **12**(1) DOI: 10.1186/1471-2105-12-124.
130. Buchfink, B., C. Xie, and D.H. Huson, *Fast and sensitive protein alignment using DIAMOND.* Nature Methods, 2014. **12**(1): p. 59-60 DOI: 10.1038/nmeth.3176.
131. Nierman, W.C., et al., *Genomic sequence of the pathogenic and allergenic filamentous fungus Aspergillus fumigatus.* Nature, 2005. **438**(7071): p. 1151-1156 DOI: 10.1038/nature04332.
132. Hubley, R., et al., *The Dfam database of repetitive DNA families.* Nucleic Acids Research, 2016. **44**(D1): p. D81-D89 DOI: 10.1093/nar/gkv1272.
133. Heng, L., *Aligning sequence reads, clone sequences and assembly contigs with BWA-MEM.* arXiv:1303.3997, 2013 DOI: 10.48550/arXiv.1303.3997.
134. Li, H., et al., *The Sequence Alignment/Map format and SAMtools.* Bioinformatics, 2009. **25**(16): p. 2078-2079 DOI: 10.1093/bioinformatics/btp352.
135. van Arkel, A.L.E., et al., *COVID-19–associated Pulmonary Aspergillosis.* American Journal of Respiratory and Critical Care Medicine, 2020. **202**(1): p. 132-135 DOI: 10.1164/rccm.202004-1038LE.

136. Danecek, P., et al., *The variant call format and VCFtools.* Bioinformatics, 2011. **27**(15): p. 2156-2158 DOI: 10.1093/bioinformatics/btr330.
137. Ortiz, E.M., *vcf2phylip v2.0: convert a VCF matrix into several matrix formats for phylogenetic analysis. (v2.0).* in *Zenodo*. 2019.
138. Stamatakis, A., *RAxML-VI-HPC: maximum likelihood-based phylogenetic analyses with thousands of taxa and mixed models.* Bioinformatics, 2006. **22**(21): p. 2688-2690 DOI: 10.1093/bioinformatics/btl446.
139. Ciccarelli, F.D., et al., *Toward Automatic Reconstruction of a Highly Resolved Tree of Life.* Science, 2006. **311**(5765): p. 1283-1287 DOI: 10.1126/science.1123061.

1365 **Supplementary Figures**

1366 **Fig. S1.**

1367 Disc diffusion screening of the PD-47 collection of isolates (Table S1 in
1368 https://doi.org/10.5281/zenodo.7021623) on RPMI plate with 10 µL of 0.8 mg/mL voriconazole. Only
1369 5 isolates could grow colonies in the inhibition halos. Upon re-inoculation of the colonies of the halo
1370 (grown in the absence or presence of voriconazole, as detailed), PD-254, PD-256 and PD-266 covered
1371 the entire plate. As explained in the text those strains were classified as resistant or heteroresistant.
1372 In contrast, PD-9 and PD-104 CoHs showed upon re-inoculation the same level of growth as the
1373 original isolates. These strains were classified as persisters.

1374 **Fig. S2.**

1375 **A)** The standardized E-test strip provided the same results as disc diffusion assays: the persister
1376 isolates PD-9 and PD-104 developed colonies in the halo of inhibition, and the non-persister isolates
1377 ATCC46645 and PD-60 did not. E-test was performed according to Biomerieux instructions and
1378 repeated three independent times. **B)** Two CoHs from PD-9 and PD-104 were picked and sequentially
1379 passaged on PDA without drug. Every second passage the spores were inoculated in a new disc
1380 diffusion assay to check the level of resistance (diameter of the halo) and persistence (appearance of
1381 colonies in the halo). After 7 passages both CoHs from both isolates showed the same level of
1382 persistence, demonstrating that this phenotype is stable.

1383 **Fig. S3.**

1384 Disc diffusion screening of the PD-47 collection of isolates. Three days after inoculation, the disc
1385 containing voriconazole (10 µL of 0.8 mg/mL) was substituted for another one containing *Aspergillus*
1386 minimal medium. A few colonies were able to grow colonies in the halos after the switch, suggesting
1387 that a few conidia remain viable. Only three strains PD-9 and PD-104 and PD-259 grew colonies before
1388 the switch. Of those, only PD-9 and PD-104 grew additional colonies after the switch.

1389 **Fig. S4.**

1390 Independent repetitions of the experiment shown in Figure 1B. The wells of 1X, 2X and 3X MIC of
1391 voriconazole for the isolates ATCC, PD-9, PD-60 and PD-104 were imaged under the microscope. The
1392 non-persister isolates ATCC and PD-60 only displayed limited microscopic growth at 1X MIC. In
1393 contrast, the persister isolates PD-9 and PD-104 displayed microscopic growth at 1X, 2X and 3X supra-
1394 MIC concentrations. Scale bar= 132.5 µm.

1395 Fig. S5

1396 **A)** Photos taken at the site of ATCC conidia inoculation on an RPMI agar plate showed that germlings
1397 are visible after 8h of incubation at 37 °C, and short hyphae have developed after 16 hours of
1398 incubation. Agar was cut out an inverted on a cover slip containing a drop of PBS. Images were taken
1399 on a Leica SP8 inverted microscope. Images were processed using Fiji [119]. **B)** There was no difference
1400 in the germination rate or ratio of the isolates ATCC, PD-9, PD-60 and PD-104. **C)** Measurement of
1401 growth rate of persister and non-persister isolates on solid RPMI showed that the strains have no
1402 difference in basal growth. **D)** Measurement of growth rate of persister and non-persister isolates on
1403 liquid RPMI showed that the strains have no difference in basal growth.

1404 **Fig. S6.**

1405 Disc diffusion screening of the PD-47 collection of isolates (Table S1
1406 https://doi.org/10.5281/zenodo.7021623) on RPMI plate with 10 µL of 3.2 mg/mL itraconazole.
1407 Isolates RC (as expected) and PD-256 did not form an inhibition halo, reflecting that they are resistant
1408 to itraconazole. Isolates PD-104 and PD-266 could grow colonies in the halo. PD-104 formed upon re-
1409 inoculation a halo of the same size and similar number of CoHs as the original isolate, suggesting that
1410 it is persistence to itraconazole. The isolate PD-266 nearly covered the inhibition halo upon
1411 reinoculation, suggesting an increment in its MIC and therefore that it is likely heteroresistant to
1412 itraconazole, as previously described for voriconazole.

1413 **Fig. S7.**

1414 **A)** MICs of itraconazole and isavuconazole for the isolates ATCC, PD-9, PD-60 and PD-104, as calculated
1415 by broth dilution assay. **B)** The isolates PD-9 and PD-104 displayed some microscopic growth at 2X the
1416 MIC concentration for both azoles, whilst the isolates ATCC and PD-60 did not grow at all and only
1417 resting conidia could be found. **C)** The entire content of the wells containing the highest concentration
1418 (8 µg/mL) if each azole were inoculated on PDA plates and incubated for 48 h at 37 °C. A noticeable
1419 ratio of viable conidia were detected for the isolates PD-9 and PD-104. Each experiment was repeated
1420 twice independently. The graph represents the means and SD

1421 **Fig. S8.**

1422 **A)** A nylon membrane was placed on the RPMI plate. Conidia were inoculated on the membrane and
1423 the disc containing voriconazole (10 µL of 0.8 mg/mL) was also put on it. As in a normal disc diffusion
1424 assay, an inhibition halo was formed, inside of which the persister strain PD-104 was able to grow
1425 small colonies, but the non-persister strain A1160 was not. **B)** A network of interacting proteins was
1426 detected by STRING ($p$=1.84e-08) when using as query the 64 genes upregulated only in persistence
1427 in PD-104. Seventeen proteins related with metabolism formed a node, formed a node suggesting a
1428 specific metabolic response during persister growth. **C)** Within the 18 genes that were upregulated in

1429 all comparisons, a tight node of 6 interacting proteins, related with ergosterol production, was
1430 detected by STRING ($p$<1.0e-16).

1431 **Fig. S9.**

1432 **A)** Representative disc diffusion plates carried out with the collection of isolates from the TAU medical
1433 centre. Six isolates were able to form CoHs, which did upon reinoculation form halos of the same size
1434 (MIC did not increase) and create a similar number of CoHs. **B)** Survival curves of larvae infected with
1435 $10^4$ or $5\times10^4$ conidia of the isolates ATCC, PD-60 (non-persisters), PD-9 or PD-104 (persisters). All
1436 strains killed larvae at a similar rate, demonstrating that they are equally virulent. For $10^4$, three
1437 independent experiments were done with 15-20 larvae/isolate in each. For $5\times10^4$, two independent
1438 experiments were done with 10-15 larvae/isolate in each. **C)** Resazurin was added to the broth dilution
1439 RPMI plate at a 0.002% (w/v) final concentration. The plate was incubated for 24 hours in a Tecan
1440 Infinity M-Plex plate reader and fluorescence was measured every 30 minutes with an excitation
1441 wavelength of 544 nm and reading emission at 590 nm using the i-control 2.0 software. The read for
1442 each well at each time point was normalize as follows: (read well time X– read 8 µg/mL voriconazole
1443 time X)/read well at time 0. The time point with the best dynamic range of values in the 1X, 2X and 3X
1444 MIC was found to be 20 hours, which was selected to determine the metabolic activity. A value of 0.1
1445 was assigned as background and values above 1 were detected in sub-MIC (macroscopic growth). At
1446 1X MIC, a slight metabolic activity could be detected for both the non-persister ATCC and the persister
1447 isolates PD-9 and PD-104. At 2X and 3X the MIC, slight metabolic activity could only be detected for
1448 the persister isolates. The experiment was performed once with two biological replicates, the graph
1449 represent the means and SEM.

1450 **Supplementary Files** (in https://doi.org/10.5281/zenodo.7021623)

1451 **Table S1:** Collection of isolates used in this study.

1452 **Table S2:** Synonymous polymorphisms detected in the *cyp51B* gene of the isolates ATCC46645, PD-9,
1453 PD-60 and PD-104.

1454 **Table S3**: GO enrichment of genes regulated exclusively in Persistence (A1163 genome as reference).

1455 **Table S4:** GO enrichment of genes regulated in Persiter VS Low Drug (Pangenome as reference).

1456 **Table S5:** GO enrichment of genes regulated exclusively in Persistence (Pangenome as reference).

1457 **Table S6:** Proteins included in the STRING network (genes upregulated only in Persistence).

1458 **Table S7**: GO enrichment of genes regulated more in Persistence (Pangenome as reference).

1459 **Table S8:** Proteins included in the STRING network (genes upregulated more in Persistence).

1460 **Table S9:** List of environmental isolates in the UK collection. Identity of the sequenced genomes. List
1461 of the clinical isolates of the TAU collection.

1462 **Table S10:** Example of the Quast obtained to determine the quality of the assembly, using the PD-
1463 104 genome.

1464 **DataSet1:** RNA-seq results and analysis of the A1160 isolate grown in NoDrug and Low Drug.

1465 **DataSet2:** RNA-seq results and analysis of the PD-104 isolate grown in NoDrug, Low Drug and
1466 Persister, using the A1163 genome as reference for the alignment of reads.

1467 **DataSet3:** RNA-seq results and analysis of the PD-104 isolate grown in NoDrug, Low Drug and
1468 Persister, using the pangenome genome as reference for the alignment of reads.

1469 **Video S1:** The persister isolate PD-9 pre-incubated in voriconazole resumes growth when the drug is
1470 withdrawn.

1471 **Video S2** The persister isolate PD-104 pre-incubated in voriconazole resumes growth when the drug
1472 is withdrawn.

1473 **Video S3** The non-persister isolate ATCC46645 pre-incubated in voriconazole resumes growth when
1474 the drug is withdrawn.